

COST EFFECTUAL RESOURCE PROVISIONING USING IOVMA AND SUPERLATIVE INTEGER PROGRAMMING

P.Durgadevi¹, T.Chindrella Priyadharshini², M.Swarnalatha³

¹Research Scholar, Anna university, Tamilnadu, (India)

^{2,3}Assistant Prof, IT Dept, RMKCET, Puduvoyal, Tamilnadu,(India)

ABSTRACT

Cloud computing is networking technology in which set of resources are provided as services. Resource allocation in cloud computing is done based on client registration using services present in cloud computing. In resources allocation there is lot of query patterns for each client for acquiring the resources i.e. memory Consumption, CPU exploitation, and other resources are usage capabilities in cloud computing. For resource provisioning in cloud two mechanisms are used. 1) Reservation and 2) on-demand plan services. In terms of cost estimation process in the cloud there is challenging task in optimization of capacity utilization in deploying virtual machine placement assignment. In this paper, we proposed an Enhanced Optimal Virtual Machine Assignment Algorithm to implement resource provisioning operations. The proposed IOVMA Algorithm makes a decision process on cloud service provider and superlative integer programming to allocate resources from cloud service providers. These service professional accepts the cloud computing services with resource provisioning with suitable services. Our experimental results shows resources are provided with minimum cost constraints in emerging cloud computing environments.

Keywords: *Networking, Superlative Integer Programming, Virtual Machine, On-Demand, Reservation.*

I INTRODUCTION

Cloud Computing is a general term used to describe a new class of network based computing that takes place over the Internet, basically a step on from Utility Computing [1]. The word service in cloud computing is the concept of being able to use reusable, components across a third party server. Without using hardware and software the third party servers providing services according to the client requirement.

A number of characteristics define cloud data, applications services and infrastructure:

- a. **Remotely hosted:** Services or data are hosted on remote infrastructure.
- b. **Ubiquitous:** Services or data are available from anywhere.
- c. **Commodified:** The result is a utility computing model similar to traditional that of traditional utilities, like gas and electricity - you pay for what you would want!

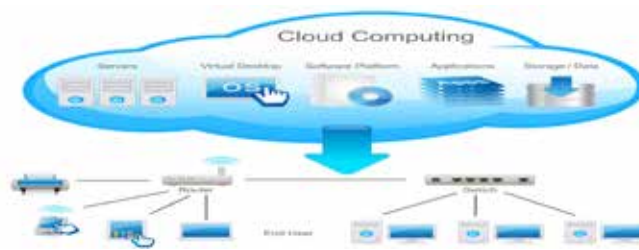


Fig.1 Cloud computing architecture

1.1 Allocation of Resource in Cloud Computing

In cloud computing, resource provisioning is an important issue as it dictates how resources may be allotted to a cloud application such that service level agreements (SLAs) of applications are met [2] .

Resource provisioning is based on FCFS scheduling algorithm, it analyzes response time distribution. This in turn is used to develop a heuristic algorithm, it defines an allocation scheme and it requires small number of servers. In responding to the effectiveness of the algorithm specification was evaluated in range of operating conditions[3]. A new modification called randomly dependent priority. It is originated to have the best performance in terms of required number of servers.

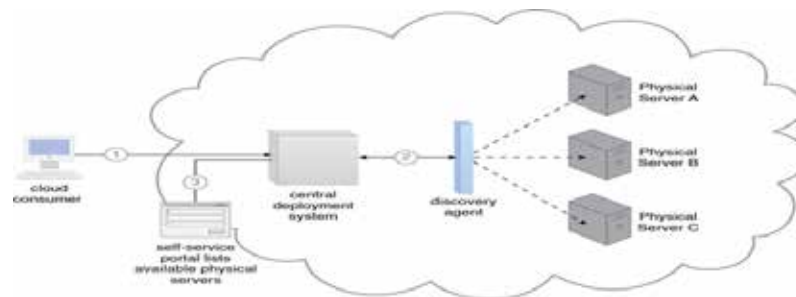


Fig.2 Allocation of resources in cloud environment

Five types of virtual instances are offered by Amazon EC2, each instance is attributed with different capacities in terms of RAM size, CPU capacity and I/O bandwidth [5] [9]. The declared volume details are virtual instances on EC2. To address fault- tolerance, EC2 distributes its virtual instances across several data centers, each data center is called as a availability zone [5][7]. To execute in different data centers, two virtual instances are running on different zones. There are six available zones, four are located in U.S. and the other two are in Europe. Further, to determine that the similar performance characteristics appear on different types of virtual instances as well, we also partially benchmark medium instances with high CPU.

1.2 Consequences of resource provisioning

As we noticed that not all small instances behave similar when serving CPU-intensive and disk I/O intensive

workloads, we further notice this phenomenon and run the third group of experiment to verify if the CPU and disk I/O performances are interlinked on evidently matching small instances. Single virtual instance performances over CPU and IO are depicted by each point. Correlation between the respective CPU and I/O performances is not observed. To process different types of workloads, different types of small instances on Amazon EC2 may be apt [9] [10]. The above literature provided about discussion of the resource provisioning operations. We describe the efficiency in the resource provisioning of the cloud computing. An Enhanced optimal virtual machine Assignment (IOVMA) algorithm is proposed for providing the resources for VMs based on two provisioning schemes: reservation and on-demand. It can adjust the transaction between the advance reservation of resources and the allocation of on-demand resources. In addition, an IOVMA also takes the demand and price uncertainties into the resource provisioning. To further improve the IOVMA algorithm, authors of the IOVMA algorithm was proposed another optimal cloud resource provisioning algorithm, called the OCRP algorithm[6]. The OCRP algorithm extends the IOVMA algorithm to provision resources for VMs in multiple provisioning stages. To solve the optimal resource provisioning in an efficient way, two different approaches Benders decomposition and sample-average approximation are applied in the OCRP algorithm instead of the SIP model. For each VM, the placement information only indicates which cloud provider hosts the VM, not the information about the located PM.

1.3 Virtualisation

Virtual workspaces is an abstraction of an execution environment that can be made dynamically available to authorized clients by using well-defined protocols, Resource quota (e.g. CPU, memory share), Software configuration (e.g. O/S, provided services). It provide infrastructure API for Plug-ins to hardware/support structures

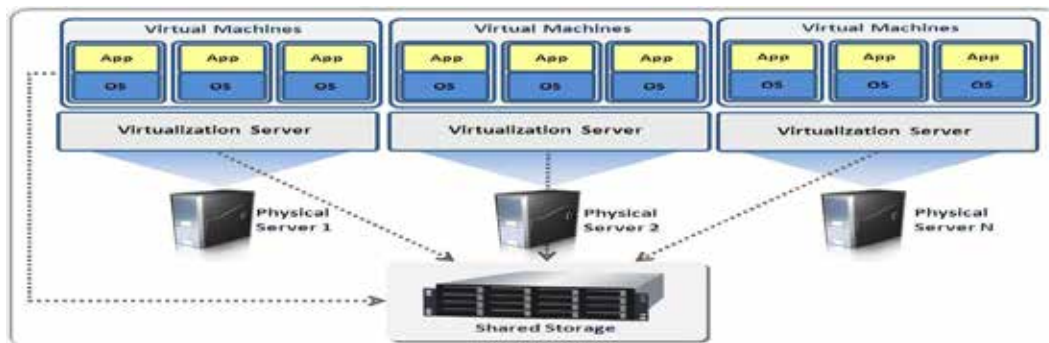


Fig.3 Virtualisation-Overview

Implementing Virtual Machines (VMs) as

- Abstraction of a physical host machine,
- Hypervisor intercepts and emulates instructions from VMs, and allows management of VMs,
- VMWare, Xen, etc.

II PRECEDING WORK

We define, the system mode that is used in this paper. Furthermore, we also review the previous studies related to our investigated Resource provisioning problem. For the VM placement issue, it has been discussed in a lot of literature. In the literature, the VM placement problem is usually transformed to the 0-1 knapsack (bin packing) problem. With the problem transformation, the PLP model corresponding to the VM placement can be easily formulated. Based on the derived PLP model, the optimal solution of the VM placement problem can be obtained [8] [10]. However, the previous VM placement literature focused on how to maximize the resource utilizations of PMs in the creation of VMs.

The amount of VM interference cost depends on various factors, such as the types of applications running in VMs, the number of VMs placed at the same PM, the choice of the VM scheduling algorithm.

2.1 PLP Representation

The PLP is a known mathematical method for solving the optimal problems with following characteristics: a linear objective function, a number of linear constraints, and an integer solution set. This model could be follow following assumptions. The cloud provider would like to create a number of new VMs in PMs concurrently [4] [5]. If the rent VM of a user cannot provide the computing environment to meet the QoS requirement of the user application, the cloud provide will return an amount of money to the user. Before placing the new VMs, each PM already has held a certain number of existing VMs. In the PLP model, after placing the new VMs in PMs, the primary function is to maximize the profit of the cloud provider.

According to the process of the virtual machine placement in commercial cloud computing, consider the cost approach for resource provisioning introduce IOVMA algorithm. Finally, VMs will be hosted in a computational environment which can be activated by third party sites termed as cloud providers. Regarding services of the cloud computing applications cloud service provider provides two types of planning services to the end users. Those services can be offered by the environment assurance in commercial cloud websites. Those are EC2, Go Grid, etc. These services are instance services and offer both reservation and on-demand plans to the end users. Generally, cost for resources in reservation scheme is less than that of on-demand scheme.

III BACKGROUND WORK

Mathematical translation of our problem statement is as follows: There are 'M' physical machines and the resource capacities of memory, CPU and Network bandwidth dimensions are provided. 'N' virtual machines are to be placed [9] [11]. We need to identify mapping between VMs and PMs that satiates the VMs' resource requirements simultaneously curtailing the number of physical machines under use.

Resource demands are predicted at regular intervals using resource demand data. These predicted values are used by a placement module to compute VM to PM mappings. This module uses first fit approximation. Extracting each individual physical machines can be considered as bins having different dimensions in virtual machine placement. These dimensions are accessed in real time data processing with virtual machine object representation and other data elements along with client requirement specification in different dimensions. We have to define behavior of the each

virtual machine placement with accurate resource generation. Resource allocation is the main achievement in optimized data delivery to clients according their requirements. Hence, due to the similarities of our problem with the bin -packing problem, we have adopted techniques like Superlative Linear Programming and First Fit which are typically used to solve traditional bin-packing problems, to solve our problem of VM Placement.

IV ALGORITHM ANALYSIS

Inputs for the algorithms include resource needed by each virtual machine to be allocated. We define a requirements matrix in order to capture these requirements through various placements with virtual organizations. The matrix is described as follows:

$$\text{Requirements Matrix: } \{r_{11}, r_{12} \dots r_{1d}\}.$$

Consider the above representation where each R_{ij} represents the requirement of VM i long as the dimension j .

Currently, we consider three dimensions for our purposes: CPU, Memory and Network bandwidth use [4] [5] [6]. Requirements along these dimensions are expressed as fractions of the total capacity of a PM.

4.1 Superlative Linear Programming

Although we believe that this particular prototype is valuable, there are three important knapsacks: the storage options under each dataset is not systematic, that is, we are not allowed to specify a preferred storage option; since each dataset is analyzed in isolation the best global solution is not obvious; and the computational specifications (number of application runs, cost per hour, machine speed, etc.) are not considered.

$$\text{Insert Equation } (x + a)^n = \sum_{k=0}^n \binom{n}{k} x^k a^{n-k}$$

Basically, the cloud provider would like to make PMs hold VMs as many as possible to generate more revenue. As increasing the number of VMs in a PM, it may introduce more interference among the VMs in the same PM. This will possibly increase the penalty payment of the cloud provider in the VM provisioning.

We are making an attempt to address these knapsacks so that we can obtain a solution to global data allocation that balances the cost and performance of both storage and computation [11]. If the best storage service for a single dataset that reside in the cloud does not have good options for the rest of the application data, then we may arrive to a sub-optimal allocation of data. As we will show, trying to find an optimal solution, that convolutes the problem to NP hard. We try to provide a ubiquitous model for this data allocation problem and a software implementation that is both fast and scalable.

V PERFORMANCE ASSESSMENT

The Enhanced Optimized Virtual Machine Assignment performed over the following parameter settings. In each PM, there have been a number of existing VMs in it. The number of the existing VM is randomly determined from 0 to 10 [5] [7]. With holding different existing VMs, the amount of available resources in each PM is also different. The amount of available resources is represented as a triple-tuple (available CPU GHz, available memory space in GB, available storage space in GB). The resource interval [(12, 129, 200), (96, 3000, 9600)] is used to randomly

decide the available resources of each PM. In each PM, it uses a 40Gbps transmission line to connect with the corresponding switch. Next, a number of new VMs is assumed to be created within 250 PMs. The number of new VMs is set from 100 to 500 in each simulation run, respectively. The amount of the resources required for a new VM was set by referring to the Amazon EC2 with 12 different resource demands [7] [8] [9]. In simulation experiments, we also refer to Amazon EC2 to set the price of each VM type and the QoS requirement of an application running in a VM. If the QoS violation is decided, the penalty payment is set using the violation ratio \times the price of the VM.

For the number of VMs created in the PMs, all the four algorithms have similar simulation results. Basically, the least fit algorithm can fully exploit the resources of PMs since it attempts to place the VM at the PM with few resources. Therefore, the least-fit algorithm should have better performance in the number of VMs created than the other two intuitive algorithms and our proposed heuristic algorithm. In the proposed OVMP algorithm, it also attempts to place many VMs to reducing the VM interference for maximizing the profit of the cloud provider.

VI EXPERIMENTAL RESULTS

We define the resource provisioning in cloud with description of all the resources. Compute or design all the relations of cloud computing.

6.1 Evaluation of Resource Allocation

In this evaluation process of extraction of various applications in cloud resource provisioning operations.

6.2 Cost Estimation

Based on the various operations present in the cloud computing environment, We describe the cloud service provider by analyzing the IOVMA algorithm with suitable consideration on reservation and on-demand cost estimation in real time virtual machine placement and in real time cloud environment. Yet, reserving too many VMs may not be optimal. Therefore, the balance between on-demand and oversubscribed costs needs to be obtained in which IOVMA performance is optimal.

6.3 Implementation

To represent long term planning we are using the IOVMA algorithm that can be applied to multiple provisioning stages. Optimal solution of the first provisioning stage depends on multiple probability and randomly distribution with consideration of occurring in sequential time operations. Multiple stages with planned and achievement releases with suitable examples. For example consider the systematic data events dynamically high efficiency various time periods in a year (e.g., Christmas Day, Valentine's Day, etc.) [2][9]. The use of decomposition method for IOVMA has to be carefully considered, since the formulation of the IOVMA algorithm is a pure integer program which is the NP-hard problem. Even though the sub problems can be solved simultaneously, the master problem with the additional Benders cuts requires considerable computational time.

An Enhanced optimal virtual machine Assignment(IOVMA) algorithm is proposed in order to reduce the total cost

due to buying reservation and on-demand plans of resource provisioning. IOVMA algorithm helps to make a decision to host a certain number of VMs on appropriate cloud providers for providing IAAS. Randomness of future demands and prices of resources are considered to optimally adjust the tradeoff between on-demand and oversubscribed costs [10] [11]. The decision made by IOVMA algorithm is obtained as the optimal solution from Superlative integer programming (EIP) formulation with two- stage recourse. Extensive derivation of mathematical models and simulation in cloud computing environment are performed to examine the effectiveness of IOVMA algorithm. The results show that IOVMA algorithm can minimize the total cost, while satisfying requirements of both providers and customers.

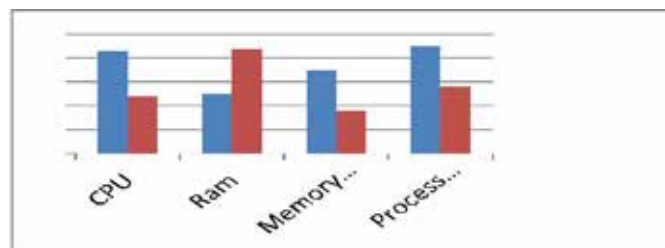


Fig. 4 Simulated result of comparison with OCRP & IOVMA

The OCRP formulates the significance of the other processors and other data management services take same environmental situation [7] [8]. the loading time other institutions are achieved in real time data passing between operating services present in cloud computing. The IOVMA procedure gives efficient and excellent improvement of the resource provisioning processing of resource like CPU and other devices present in cloud computing operations

VII CONCLUSION

Solving Superlative integer programming with multistage recourse will result in the optimal solution. PIP is obtained from OCRP. Benders decomposition approach to divide an OCRP problem into sub problems which can be solved parallels is also applied. An Enhanced optimal virtual machine placement (IOVMA) algorithm is proposed in this paper, this algorithm can be extended to implement optimized resource provisioning operations. This algorithm could reduce the cost spent in each plan for hosting virtual machines in a multiple cloud provider environment with future demand and price uncertainty.

REFERENCES

- [1] Introduction to Cloud Computing, Fact Sheet, Fiche d'information
- [2] "Resource Provisioning for Cloud Computing", IEEE International Conference on Autonomic Systems, Barcelona, 2009, Ye Hu1, Johnny Wong, Gabriel Iszlai, and Marin Litoiu,
- [3] "Efficient Resource Provisioning in Compute Clouds via VM Multiplexing", ICAC'10, June 7–11, 2010, Washington, DC, USA. Copyright 2010 ACM 978-1-4503-0074-2/10/06 ...\$10.00, Xiaoqiao Meng, Canturk Isci, Jeffrey Kephart, Li Zhang, Eric Bouillet,
- [4] "SLA-Oriented Resource Provisioning for Cloud Computing: Challenges, Architecture, and Solutions ", Rajkumar Buyya, Saurabh Kumar Garg, and Rodrigo N. Calheiros, 2011 International Conference on Cloud and

Service Computing, 978-1-4577-1637-9/11/\$26.00 ©2011 IEEE.

- [5] "Optimization of Resource Provisioning Cost in Cloud Computing", Sivadon Chaisiri, Bu-Sung Lee, IEEE Transactions On Services Computing, Vol. 5, No. 2, April-June 2012.
- [6] "Optimal Virtual Machine Placement across Multiple Cloud Providers," S. Chaisiri, B.S. Lee, and D. Niyato, Proc. IEEE Asia-Pacific Services Computing Conf. (APSCC), 2009.
- [7] "Profiling Energy Usage for Efficient Consumption," R. Chheda, Stokowski, S. Stefanovich and J. Toscano, Architecture J., no. 18, 2008. "SLA-Aware Virtual Resource Management for Cloud Infrastructures," H.N. Van, F.D. Tran, and J.-M. Menaud, Proc. IEEE Ninth Int'l Conf. Computer and Information Technology, 2009.
- [8] "The FEDERICA Project Website," <http://www.fp7-federica.eu>, 2013.
- [9] D. Andersen, "Theoretical Approaches To Node Assignment," Unpublished Manuscript, <http://www-cs.cmu.edu/~dga/papers/andersen-assign.ps>, 2002.
- [10] M. Yu, Y. Yi, J. Rexford, and M. Chiang, "Rethinking Virtual Network Embedding: Substrate Support for Path Splitting and Migration," *ACM SIGCOMM Computer Comm. Rev.*, vol.38, no. 2, pp. 17-29, Apr. 2008, doi:10.1145/1355734.1355737.
- [11] W. Szeto, Y. Iraqi, and R. Boutaba, "A Multi-Commodity Flow Based Approach to Virtual Network Resource Allocation," Proc. IEEE GLOBECOM '03, vol. 6, pp. 3004-3008, Dec. 2003, doi:10.1109/GLOCOM.2003.1258787.
- [12] J. Fan and M.H. Ammar, "Dynamic Topology Configuration in Service Overlay Networks: A Study of Reconfiguration Policies," Proc. IEEE INFOCOM '06, pp. 1-12, Apr. 2006, doi:10.1109/INFOCOM.2006.139.
- [13] J. Lu and J. Turner, "Efficient Mapping of Virtual Networks onto a Shared Substrate," Technical Report WUCSE-2006-35, Washington Univ. St. Louis, 2006.
- [14] Y. Zhu and M.H. Ammar, "Algorithms for Assigning Substrate Network Resources to Virtual Network Components," Proc. IEEE INFOCOM '06, pp. 1-12, Apr. 2006, doi:10.1109/INFOCOM.2006.322.

DECENTRALIZED VARIATIONAL CLUSTERING ALGORITHM FOR TARGET TRACKING IN HYBRID SENSOR NETWORK USING PARTICLE SWARM OPTIMIZATION

A. Arun Kumar¹, J. Rejina Parvin²

¹ PG Scholar, Department of ECE, Dr. N G P Institute of Technology, Coimbatore (India)

² Assistant Professor, Department of ECE, Dr. N G P Institute of Technology, Coimbatore (India)

ABSTRACT

In target tracking, Wireless Sensor Networks are used to track the target to find its mobility of the nodes in order to improve the performance of the network. In the existing system, target tracking is done with the help of static sensor nodes with few dynamic nodes. The terms like velocity and acceleration are considered for predicting the next position of the target. In order to predict the precise information of the target's next position, in addition to the velocity and acceleration, parameters like direction and angle of direction of the target are also considered in the proposed system. The proposed method is described in two phases namely: Estimation and Prediction phase using interval theory. Further, the relocating of nodes employs the Ant Colony Optimization Algorithm. In the proposed system, static nodes ensures that coverages of the sensing area and dynamic nodes to assure the prediction of the target. Once the target next position is predicted that allowing the mobile sensor nodes to move nearer to the target. Using Particle Swarm Optimization, cluster formation takes place and the sensed information is being transmitted to the Base Station. The proposed system assures that, the minimum estimation time of the target with minimal error. Using Ns-2 simulator, the proposed system is simulated and the performance are compared with the existing system.

Keywords: *Ant Colony Algorithm, Estimation of Target's position, Interval Theory, Particle Swarm optimization, Target Tracking.*

I. INTRODUCTION

Wireless Sensor Networks (WSN) plays an important role in many applications due its advancement in recent technologies. This includes Wildlife Monitoring, Military Surveillance and Under Water Sensor Network and Surveillance. WSN refers to a large number of intelligent sensor nodes which capable of sensing, communicating the information throughout the implementation of the tasks in the specified sensing region. Mobile sensor nodes are more versatile compared with the static sensor networks as per the capability of nodes; it can be deployed in any scenario and change of cope with rapid topology.

Usually applications are similar, but variation only in the field of communication such as environment monitoring or surveillance [1]. Commonly the nodes consist of a transceiver, sensing unit and processing unit as well as powered by a battery and few sensor for detecting light, temperature, heat and humidity.

The target tracking using WSN environment shows similarity with energy constraint, since the sensor nodes have limited power and computational capability which may not be sample for the complex in traditional target tracking [2]. The typical schemes of hierarchical are four categories under WSN environment that includes dynamic and distributed tree-based tracking, RFID-based tracking, prediction-based tracking and peer to peer tracking. Target Tracking is a typical WSN application that to sense the target at particular times which are kept in active mode and remaining other nodes are maintained inactive. So that it consists of energy will be maintain at each sensor node. The continuity of monitoring mobile target must be turned ON just before the target reaches to them. In similar cases, there are several issues that should satisfy the limitation of the performance of WSN. First of all, the sensor nodes should be deployed properly in the sensing region before tracking the target [2] [3]. In [4] [5], defines the sensor coverage model. Second, the long distance communication is to be totally avoided before the process of communication of each node.

The major two technologies under WSN environment can be categorised into wireless communication and MEMS which have the way of result in the development of Wireless Sensor Networks. These provide relatively inexpensive sensor nodes which are capable of gathering, processing and storing as well as transferring information between each node. These nodes gathering information from a network through which sensor reading can be implemented. Therefore the intelligence sensor nodes have to sense the data that can be processed and transmitted to the Base Station (BS). In a flurry of research activities, the flexibility of installation and configuration are the key factor in which performing the improved result. In the area of sensor networks, a nodes gathering information and acceptance can be done in the field of industries such as telecommunication, security of information and automobile techniques.

Especially in the purpose of military application and other information security task, the monitoring area is not so much usually protected in WSN. For better performance, the deployment information provides the good option to key management scheme for WSN that gives encoding and decoding information.

The sensor can be deployed accordance with the key features of information based on the sensing area. The sensor deployment can be three types [6] namely 1) Triangular sensor deployment, 2) square sensor deployment and 3) irregular sensor deployment.

The rest of the paper is organizes as follows. Related works and the Experimental set up of the proposed system are explained in section II and section III respectively. The proposed work is compared with existing system and discussed in section IV. Finally, the conclusion and scope for future work are given in section V.

II. RELATED WORK

Many of the research are being carried out related to Wireless Network scenario. But in some case the target tracking needs a platform to estimate the current position of a single target. Based on the scheme of target tracking using WSN environment, the probability of predicting the target can be explained as follows.

2.1 Controlled Mobility Sensor Network

In this paper [7], a novel strategy for managing sensors mobility is desired, which aims at improving the estimation of current position of a single target. The method consists of four sequential phases based on the each iterate time step as follows:

- First to estimate the current position of the target,

- After that, the targets next position can be predicted with the help of current and previous position location,
- In estimation process, to computing a set of new location to be taken by mobile nodes,
- Finally, assigning new location for the nearby mobile sensor node within the region of computed set using Ant Colony Optimization (ACO) algorithm.

There are two phases that provides the variation of solving the consecutive phase that iterate each time step.

1. Estimation phase
2. Optimization phase

Estimation Phase

By resolving the estimation phase using interval analysis [8] can be performed. For predicting the targets next position the region of interest which can be covered.

Optimization Phase

Optimization can be done using Ant Colony Optimization algorithm (ACO) to relocate the mobile sensor nodes nearer to the target. In other words, it can able to accomplish the complex operational research problem. While moving the sensor nodes, the total coverage of the network can be limited energy constraints.

The entire network can be covered by sensors in order to accomplish the intruders. For this purpose, static and dynamic nodes are the two sensors which can be used for the purpose of target tracking. Mobile sensors are used to improve the performance and static sensors to ensure that a continuous coverage of the network sensing region.

2.2 Interval Based Estimation

For solving the estimation problem, the interval analysis can be used. Let us consider the interval denoted as $[y_1]$ and $[y_2]$ is a closed subset of IR given in [9]:

$$[y] = [y_1, y_2] = \{y \in \mathbb{R} \mid y_1 < y < y_2\} \quad (1)$$

For the nth interval [10], the two dimensional equation of y can be given by

$$[y] = [y_1] * \dots * [y_n] \quad (2)$$

The set of all arithmetic operation having several applied intervals of closed subsets [10] which follow on Table I:

Table I
Set of all Arithmetic Operation Applied to Intervals

Operators	Definitions
+	$[x] + [y] = [x_1 + y_1, x_2 + y_2]$
-	$[x] - [y] = [x_1 - y_2, x_2 - y_1]$
\cap	$[x] \cap [y] = [\max\{x_1, y_1\}, \min\{x_2, y_2\}]$
\cup	$[x] \cup [y] = [\min\{x_1, y_1\}, \max\{x_2, y_2\}]$

Relocation of the Mobile Sensor

In order to move the sensor nodes to assure better coverage area and also to predict the targets next position mobile sensor nodes are used. In this concept, the relocation takes place of such mobile nodes to ensure the regular sensing of the target. ACO is used for relocating the nodes.

III DISTRIBUTED ENERGY OPTIMIZATION

In order to improve the performance in target tracking, the energy consumption is desired to be optimized [11]. Recently, the research has mainly focused on the energy optimization and target tracking problems.

Preliminaries

Let us consider a hybrid WSN scenario comprised of static and mobile sensor nodes deployed in two dimensional sensing fields. Moreover it is assumed that each sensor has some sensing range and its location can be obtained using GPS. The performance enhancements of WSN, the static nodes are deployed randomly in advance and then placement of dynamic nodes can be done accordance in the field of sensing region. In this section II, the probability sensing coverage model for reliability detection can be established to enhance the position information of the target.

3.1 Energy Consumption Model

Heinzelman et. al proposed that each sensor node consists of component and radio characteristics such as for sensing unit, processing unit and transceiver for transmitting and receiving data. For the availability of energy consumption in WSN, the lifetime is an important factor in energy consumption model. Due to its advancement technique, the sensors go into the sleep for long time to consume energy. Before the initial assumption or measurement, the features of radio components are discussed [12]. The radio component has two modes of operation: 1. Low Power Listening (LPL) and 2.Reception and transmission in Rx/Tx mode. Table II reproduces their model:

Table II
Radio Characteristics

Radio mode	Energy Consumption
Transmitter Electronics ($E_{TX-elec}$)	50nJ/bit
Receiver Electronics ($E_{RX-elec}$)	
Transmit Amplifier (ϵ_{amp})	100mJ/bit/m ²
Idle	40nJ/bit
Sleep	0

3.2 Dynamic Sensor Node Scheduling

A group of sensor can be selected in advance and considering accuracy and performance measure of energy consumption. After the initial measurement of each sensor nodes, the targets information can be transmitted between the selected nodes and then the group of sensor acquire the information with similar nodes transmit them to a cluster heads. According to this section, the characteristic of radio component precedes the assumption of classic model for energy consumption.

In summary, a survey of existing technique is related to Hybrid Wireless Sensor Network for target tracking application, involving sensor deployment, interval analysis and sensing energy management.

IV PROPOSED SYSTEM

A target tracking system through WSNs can have several advantages a) qualitative and mobility observations b) signal processing accurately and data acquisition c) increased tracking system, robustness and accuracy. While, the use of sensor networks for target tracking in Wireless Sensor Network provides a number of new innovative challenges [1]. These challenges include limited energy supply and communication bandwidth through the control of distributed algorithms, and handling the limitations and fundamental performance of sensor nodes, especially the target tracking based on the size of the network becomes it gives large number of nodes to cover up the sensing region.

As sensor networks are typically used to monitor the environment, especially it gives a fundamental issues is the location-tracking problem that provides a goal to trace the roaming paths of moving nodes or objects in the specified area of coverage region. In order to that, it forms a disadvantage which is used in target tracking applications. Thereby, once all the sensor nodes deployed in the sensing region it follows:

1. All the nodes are in active mode,
2. Start to sense the target,

If Target entering into the sensing region and all the nodes get listening to the target, Only there are few nodes nearer to the target, all nodes remain active it causes:

- Results in early node failure
- It can make other sensor nodes to sleep

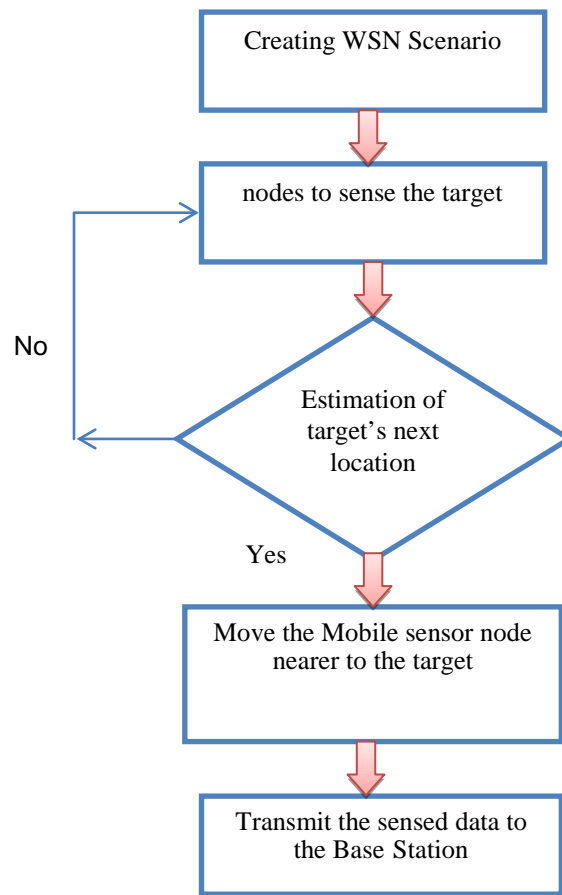


Fig.1: Flow Diagram of the Proposed System

The above Figure 1 illustrates the Flow diagram of the proposed system, which initializes the static and dynamic nodes for target tracking in Hybrid Sensor Network. After initialization, the static and dynamic nodes are deployed in the coverage region to sense the data and being to predict the targets next position. In order to that, cluster formation can be formed using Particle Swarm Optimization (PSO) algorithm and then finally, sensed data send to the base station.

4.1 Reliable Detection Model

The sensing coverage model [11] is assumed that all the sensor nodes have sensing range s_r that is in the form of Δ . s_r ($\Delta < 1$) if Δ denotes the uncertainty sensing range of each sensor node i . if the coordinates of sensor node and target are given by (a_i, b_i) and (a_{target}, b_{target}) respectively. Then the reliability detection probability (dp) is given as

$$dp = 1 - \prod (1 - di) \tag{3}$$

Where dp is the reliability detection probability of sensor node i on the target and which is given as follows:

$$d_i = \begin{cases} 0, & d_{target,i} / sr \geq 1 + \Delta \\ e^{-\frac{\alpha_1 d_{target,i}}{\alpha_2 sr}} \cdot \alpha_2, & 1 - \Delta < d_{target,i} / sr < 1 + \Delta \\ \alpha_2, & d_{target,i} / sr \leq 1 - \Delta \end{cases} \quad (4)$$

Whereas $d_{target,i}$ is the distance between sensor node i and the parameter λ_1 and λ_2 are calculated as

$$\begin{aligned} \lambda_1 &= sr \cdot (\Delta - 1) + d_{target,i} \\ \lambda_2 &= sr \cdot (\Delta + 1) - d_{target,i} \end{aligned} \quad (5)$$

Therefore, the detection of target can be based on the reliable detection probability of each sensor i . Moreover, target and collaborative sensing model gives the way of finding the targets location in two dimensional sensing fields with maximum speed and acceleration constructed by Yang and Feng [13]. The motion model of target tracking is performed by the sink node [14]. With the help of predicted target location, hereby applying the potential scheduling scheme can be performed on the sensor nodes.

5.2 Estimation of Target Sensing Model

After the detection of target using reliable probability model, the targets next position with the help of acceleration, velocity and angle should be provided and the position information to be taken according to the specified sensing period.

Let $x(1), \dots, x(n)$ be all available estimated positions of the target. Then, a k^{th} order of prediction model in estimation process is given in the equation 6:

$$x_1(t+1) = f(x(t) \dots x(t-k)) \quad (6)$$

Where f is the prediction function and $x_1(t+1)$ is the predicted position of the target regarding time $t + 1$. The equation (6) gives available information about the target motion could be used to refine the prediction model. Then it gives second order prediction model as follows in the equation 7:

$$x_1(t+1) = x(t) + \Delta t \cdot v(t) + \Delta t^2 / 2 \cdot \gamma(t) \quad (7)$$

Where

Δt - time period between two following time-steps and

$v(t)$ and $\gamma(t)$ - respective estimate vectors of the instant velocity and the instant acceleration at time t .

The velocity acceleration of time interval 't' given in the equation 8:

$$\begin{cases} v(t) = \frac{x(t) - x(t-1)}{\Delta t} \\ \gamma(t) = \frac{v(t) - v(t-1)}{\Delta t} \end{cases} \quad (8)$$

In the interval framework [7], the prediction model is formulated as follows in the equation 9:

$$[x1](t + 1) = [x](t) + \Delta t \cdot [v](t) + \Delta \frac{\Delta t^2}{2} \cdot [y](t) \quad (9)$$

Where $[x1](t+1)$ is the predicted position box of the target, using equation (8) and (9), yields a box including the next-step position of the target. Thus the process equation can determine by the function of motion model and it can be given by

$$X^{tar}(k+1) = FX^{tar}(k) + G1U^{tar}(k) + G2V^{tar}(k) \quad (10)$$

Where X is consider as speed of the target, U is computed as ratio of acceleration and speed, V is maximum speed, K is the time index, F is the model state transition matrix and G is the coupling matrix [11].

$$F = \begin{bmatrix} 1 & T & 0 \\ 0 & 1 & 0 \\ 0 & 0 & 1 \end{bmatrix}, G1=G2 = \begin{bmatrix} T^2/2 & 0 \\ T & T^2/2 \\ 0 & T \end{bmatrix} \quad (11)$$

While predicting the target next position, the direction finding error can be obtained. If suppose, the DF error of these sensor nodes cannot be intersect at a common point due to its high Direction Finding (DF) error.

IV RESULTS AND DISCUSSION

The proposed work of Target Tracking is simulated using NS-2.32 version Simulator. In Network Simulator software, it is a Graphical User Interface (GUI). Its front end is a Tool Command Language and back end is C++.

Table III
System Specification

1.	Simulator Tool	NS
2.	Version	2.32
3.	Operating System	Linux (RedHat)
4.	Environment	GUI
5.	Front End	TCL
6.	Back End	C++

The initial network parameters considered for the simulation is shown in Table IV an initial domain, for instance the whole deployment area, is thus contracted in order to obtain the smallest box including the exact scalar solution.

Table IV
Initial Network Parameters

S.No	Parameter	Value
1.	No of Nodes	50
2.	Sensing Region	200*200 m

3.	Initial Energy of sensor node	200J
4.	Radius of cluster (r)	30m
5.	Sensing range	100m
6.	Packet size	512 bytes
7.	Transmission Power	0.02Watts
8.	Received Power	0.01Watts
9.	Packet Generation Interval	0.1Sec
10.	Transmission Rate	409Kbps

4.1 Basic Initialization and Requirements

1. Basic assumptions are made in this method such that both the target and the sensor nodes are supposed having constant velocities in which it has 25 static nodes and 25 dynamic nodes with the energy of 100 Joules.
2. The initial network parameter includes declaration of Nam window and Trace file. The Base Station is assigned in the Scenario and named as node 1 and then target's is allowed to move in the network.
3. Trace all shows that the sensing of all the nodes included in Hybrid Sensor Network which is displayed in the Nam window.

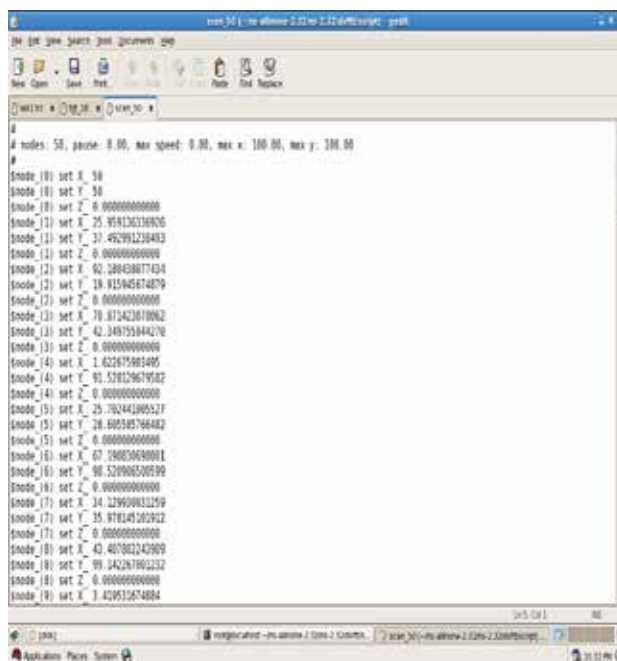


Fig.2: Position of the Sensor Nodes in the Network

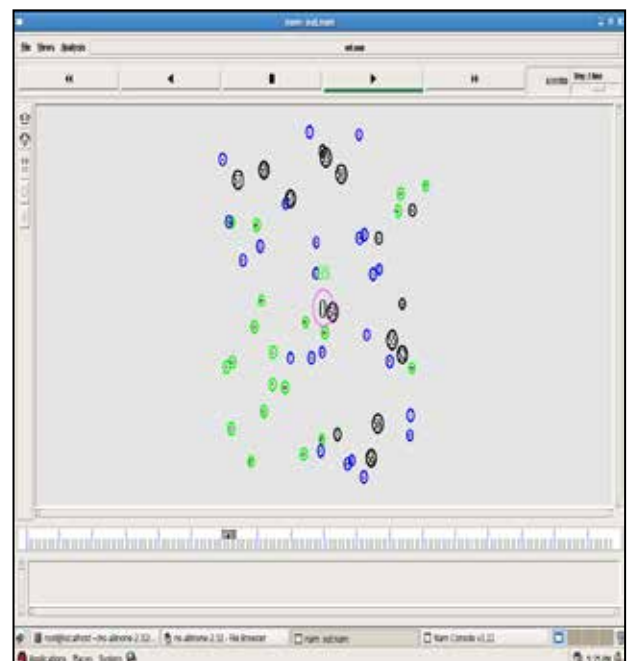


Fig.3: Simulation Output for Static and Dynamic nodes

The above Figure 2 shows the sensing data of all nodes which is displaced in coordinates that send to the base station and acquires information about the network. The coordinates x, y and z shows that the position of the each nodes, which gives the specification and deployment of the static and mobile nodes. The position of the sensor mainly focused on upgrading the topology of the network, improving the area of coverage through sensing model and increasing the lifetime of the network through limited bandwidth.

- [6] S. Shakkottai, R. Srikant, and N. Shroff, "Unreliable sensor grids: Coverage, connectivity and diameter", Twenty-Second Annual Joint Conference of the IEEE Computer and Communications Vol. 2, No.1, 2003, pp. 1073–1083.
- [7] H.-T.Kung and D.Vlah,"Efficient location tracking using sensor networks", in Wireless Communications and Networking, IEEE Journal, Vol.11, No.3, 2006, pp. 1954–1961.
- [8] L. Jaulin, M. Kieffer, O. Didrit, and E. Walter, "Applied Interval Analysis", Springer, 2001.
- [9] R.E. Moore, "Methods and Applications of Interval Analysis", SIAM, 1979.
- [10] Farah Mourad, Hicham Chehade, Hichem Snoussi, Farouk Yalaoui, Lionel Amodeo, and Cedric Richard, "Controlled Mobility Sensor Networks for Target Tracking Using Ant Colony Optimization", IEEE Transactions on Mobile Computing, vol. 11, no. 8, 2012, pp. 1261-1273.
- [11] Jing Teng and Hichem Snoussi, "Distributed Energy Optimization for Target Tracking in Wireless Sensor Networks", IEEE Transactions on Mobile Computing, Vol. 9, No.10, 2010, pp.1465-1477.
- [12] A.S. Chhetri and D. Morrell, "Energy Efficient Target Tracking in a Sensor Network Using Non-Myopic Sensor Scheduling," Proc. Int'l Conf. Information Fusion, Feb. 2005, pp. 558-565.
- [13] L. Yang and C. Feng, "Adaptive Tracking in Distributed Wireless Sensor Networks," Proc. IEEE Int'l Symp. And Workshop Eng. Computer Based Systems, Mar. 2006, pp. 103-111.
- [14] F.B. Duh and C.T. Lin, "Tracking a Manerling Target Using Neural Fuzzy Network," IEEE Trans. System, Man, and Cybernetics, vol. 34, no. 1, 2004, pp. 16-33.
- [15] R. Shorey, ed. John Wiley & Sons, "Mobile, Wireless, and Sensor Networks: Technology, Applications, and Future Directions" 2006.

A SURVEY ON INDIAN CURRENCY NOTE DENOMINATION RECOGNITION SYSTEM

Aruna D H¹, Manpreet Bagga², Dr.Baljit Singh³

¹ M.Tech Student, Dept of Computer Science, GSSSIETW Engg Mysore, India

² Associate Professor, Dept of Information Science, GSSSIETW Mysore, India

³ Associate Professor, Dept of Computer, BBSB College of Fatehgarh Sahib Punjab (India)

ABSTRACT

At present the Currency denomination recognition is becomes dynamic topic for researchers in different potential applications. Financial exchange is an essential piece of our everyday activities. But for the visually impaired individuals especially suffer in financial exchanges. They are not ready to adequately recognize different denominations and are frequently betrayed by other individuals. Hence a reliable currency recognition system could be utilized as a part of any division wherever money related exchange is of concern. Accordingly, there is a vigorous need to outline a framework that is useful in recognition of paper money notes accurately. Currency denomination detection is an immeasurable area of exploration and huge advancement had been accomplished through the years. In this paper currency recognition explored and also presented a comprehensive review of the existing literature on techniques related to Indian Currency Note Denomination Recognition, the effort of survey promotes to give the effective system for visually impaired.

Keywords: Computer Vision, Feature Extraction, Image Processing

I. INTRODUCTION

Form the past many years the currency systems are most commonly used in India. In the 1861 the Government of India presented its first paper cash issuing 10 rupee notes ,further in1864; 20 rupee notes are introduced, in 1875 ;5 rupees notes in1899 ;10,000 rupees notes in 1900;100 rupee notes in 1905; 50 rupees notes in 1907; 500 rupees notes and similarly in 1909; 1000 rupees are developed . .The Reserve Bank of India (RBI) started note generation in 1938, issuing 1000, 100, 50,20,10,5,2 rupee notes, while the Government kept on issuing 1 rupee notes. At present the currency system in India has 1,2,5,10,50,100,500,1000 Rs but these are unique in one way are other. These characteristics may be shade, size or some distinguishing proof imprints and so on. It is not difficult to perceive these peculiarities for the common people but not for the visually impaired people .These visually impaired individuals can recognize in the two separate groups utilizing the distinctive size of notes, up till now the size variety alone is insufficient to faultlessly focus the cash note. In actuality, the almost no distinction between the sizes of continuous categories makes them mystified or confused not able to recognize the cash notes from each other. The cash notes are given few exceptional distinguishing proof stamps just for the visually impaired individuals with the goal that they might effectively perceive the category accurately. Each cash note has its section impressed at the upper right end which is delicate to touch, still this

imprint blurs away after the coin note goes available for use for quite a while. This again makes a trouble for the visually impaired individuals to accurately focus the category of the coin note.

A currency recognition framework for a visually impaired people is surveyed in this paper. And also the concentrated over the benefits of the currency recognition system using a color picture. And many techniques are used to recognize the image but in many cases neural networks are used to recognize the currency notes which contains the several steps namely some texture and pattern based .The identification of the object is nothing but the recognition. This procedure would presumably begin with picture handling methods, for example removal of the noise, emulated by (low-level) characteristic extraction to place lines, and certain texture contains the texture and the certain boundaries. The shrewd bit is to translate accumulations of these shapes as single articles, e.g. autos on a street, boxes on a carpet lift or carcinogenic cells on a magnifying image instrument slide. One explanation behind this is an AI issue that an item can seem altogether different when seen from distinctive points or under dissimilar lighting. An alternate issue is of choosing what features fit in with what item and which are foundations or shadows and so on. The human visual framework performs these undertakings inadvertently. But a machine obliges skilful programming and loads of handling force to approach human execution. The remaining section as arranged is as follows: II section describes the related work of the currency recognition system.III section describes the some major steps in the currency recognition system. IV section describes the evolution in the algorithms of the currency recognition system V section describes the techniques used in the image analyses of the currency recognition system.VI sections gives the conclusion of the survey in the currency recognition system.

II. RELATED WORK

The survey has proposed by Jain [1] an image processing method to extract paper currency quantity. The extracted ROI may be wormed with Pattern Recognition and Neural Networks matching method. First they obtain the image by easy flat scanner on glue dpi with an exacting size, the pixels level is place to attain image. A few filters are useful to extract denomination assessment of note. They employ dissimilar pixel levels in different quantity notes.

The paper was presented by Mirza and Nanda [2] a technique for validating paper currency of India. The technique employs four characteristics of paper currency plus identification mark, security thread, latent image and watermark. The scheme may extract the hidden features i.e. latent image and watermark of the paper currency. The anticipated work is an attempt to propose an approach for the characteristic extraction of Indian paper currency.

The review was presented by Chakraborty et al. [3] a widespread review of study on a assortment of developments in existing years in classification of currency denomination. A number of techniques applied by a diversity of researchers are proposed briefly in organize to evaluate the condition of art. In this paper the author also focusing primarily on currency detection system including different steps involved in it like image attainment, feature extraction and categorization system uses different algorithm.

The paper was demonstrated by Reel et al. [4] of the heuristic analysis of characters and a number of serial numbers of Indian currency notes to recognition of currency notes. To distinguish a character from a given

currency image, there is require to extract feature descriptors of such image. As an extraction technique significantly affects the quality of entire OCR process, it is very significant to extract features, which will be invariant towards the different light conditions, employ font type and deformations of characters caused by a distort of the image. Heuristic analysis of characters is complete for this reason to get the precise features of characters previous feature extraction in currency recognition.

The survey was focused by Pawade et al. [5] on existing techniques and systems for currency recognition stands on image processing. They have discussed both invent recognition and paper currency recognition techniques separately. Finally they summarized their work in tabular form which is very cooperative for study at a glance. Even though there is lot of research work done on this topic, still there are a number of issues related to the accuracy and efficiency of the method. Thus achieving maximum efficiency and getting 100% correctness for heterogeneous currency, when physical state of currency is not that much good, will always be a defy for researchers.

The review was demonstrated by Ali and Manzoor [6] of the technique for currency recognition using image processing. The proposition system employs the various features of the currency for recognition. Their experiment demonstrates that this is the squat cost machine to recognize the Pakistani paper currency notes. They had checked various notes on this system and the result is 100% which means that the system is working competently.

The paper was suggested by Krishan [7] an advances for the feature extraction of Indian currency notes. An Approach suggested from the beginning of scanning a document of converting it to binary image, thresholding, and morphological filtering and word segmentation has been successfully stated. One of the dispute facades in the character segmentation part is that two characters are sometimes joined together.

The review was conducted by Danti and Nayak [8] an important feature of Indian Currency Note are extracted and recognized. Currency features such as denomination, governor declaration, year of print etc. are segmented for recognition using 3×3 grid. Stands on geometrical shape, quantity of currency such as 100, 500, 1000 are determined with the help of Neural Network classifier. Year of publish of currency note is extracted using OCR techniques. Proposed method is experimented on a large dataset and demonstrated the efficiency of the approach.

The paper was proposed by Tanaka et al. [9] of the probability solidity formed by a multivariable Gaussian function, where the input data legroom is transferred to a lower dimensional subspace. Owing to the constitution of this model, they describe the total processing system as a hybrid neural network. While the calculation of the verification model is only to take internal product and square, the computational freight is very small.

The review was presented by Malik et al. [10] a reliable coin recognition system that is stands on a polar Fast Fourier Transform. Coins are regularly employed in each and everyday lives at a variety of places like in banks; grocery stores; supermarkets; automated weighing machines; vending machines etc. Thus, there is a fundamental require to mechanize the counting and sorting of coins. For this machines require to distinguish the coins very fast and precisely, as additional transaction processing depends on this gratitude.

The paper was discussed by Pathrabe and Bawane [11] a method for recognizing paper currencies of different countries. The technique uses three characteristics of paper currencies including size, color, and template. In this

technique the system can be trained for a new denomination banknote by just introducing one intact example of the banknote to it. In calculation the system may recognize the banknote on each side or any direction.

The review was illustrated by Sannakki and Gunjale [12] on their system intend to recognize and classify the currency notes by using dissimilar steps starting from image acquisition, preprocessing, testing, and training. Methodology used for feature extraction is Discrete Wavelet Transform (DWT) and estimated coefficient matrix of the currency image is derived. Statistical features are extracted using coefficient and stored in a vector.

The paper was demonstrated by Velu et al. [13] of the perfect image of a coin is employed for learning and appreciation. The correct classification of acceptance of a coin was achieved for 99.6% in a test sample of 10,000 coins. The Robert's, Laplacian and Canny edge detection methods gives 93%, 95% and 97.25% of the coin image. The planned ML-CPNN yields 99.47% recognition rate. By analyzing the experimental results, it is evident that, ML-CPNN yields the best result. This paper may be extended to categorize coins released during various time periods. Also, stands on the coin shape, notion on the coin, and metal of the coin etc, also, the categorization may be done depends on the similarity measure of a coin and based on the size and spatial location of peaks in the parameter space.

The review was proposed by Ravi and Ravi [14] to extort the surface features of exchange note images. To extort the features; they are using PCA Algorithm. It is exploiting on a currency note and the inexact coefficient-matrix of the distorted image is obtained. A set of coefficient statistical instants are removed from the approximate Co-efficient matrix. The extracted features are amassed in a feature vector. The extracted features may be employed for appreciation, categorization and retrieval of currency notes.

The paper was demonstrated by Bhavani and Karthikeyan [15] on the efficiency of SURF for banknote recognition. The scale-invariant and rotation-invariant attention point detector and descriptor provided by SURF is robust to handle the image rotation, scaling change and enlightenment change.

The review was presented by Sargano et al. [16] a new intelligent system for paper currency recognition. Pakistani paper currency has been considered as a case study, for intelligent recognition. This paper identifies, introduces, and extracts robust features from Pakistani banknotes. After extracting these features, the paper suggests to employ three layers of feed forward reverse promulgation Neural Network for classification. The planned method and system are simple and comparatively less time consuming which makes it suitable for real-time applications.

The paper was developed by Aggarwal and Kumar [17] an interactive system which produces Currency Recognition System using Localization and Color Recognition with the help of Matlab. The Indian currency notes have been properly recognized and the quantity has been found with a high level of accuracy. This system has much progression over the existing systems and they can confirm the following observations.

- It is probable to localize the currency note and subtract it from its background.
- The system accepts the interactive techniques of Currency Localization and Color Recognition.
- The system permits the user to identify the Currency note.
- The system is exclusive in its applications.
- The efficiency of their system is 96%.

III. IMPORTANCE OF CURRENCY RECOGNITION SYSTEM

There are some important steps in the currency Recognition system as shown in the figure1 and is stated as follows.

Image Acquisition: There are different approaches to procure picture, for example, with the assistance of cam or scanner. Acquired image have to hold all the features

Preprocessing: Preprocessing operations are ordinarily needed before the fundamental information examination and extraction of data. The point of picture preprocessing is to stifle undesired mutilations or upgrade some picture offers that are essential for further preparing or investigation. It incorporates

Image Adjusting: When we get the picture from a scanner, the extent of the picture is so huge. So as to diminish the count, we diminish the span of picture. Picture Adjusting is finished with the assistance of picture introduction. Addition is the method basically utilized for undertakings, for example, zooming, pivoting, contracting, and for geometric amendments

- ✓ **Image Smoothing:** At the point when utilizing a cam or a scanner and perform picture exchanges, were some will show up on the picture. Image noise is the illogical variety of brightness in pictures. Removal of the noise is an essential step when image processing is individually performed. However this noise may affect the pattern matching and segmentation. At the point when performing smoothing process on a pixel, the neighbor of the pixel is utilized to do some changing. After the steps the new value is formed the different pixels and they develop a framework, the extent of the grid is odd number, and the target pixel is spotted on the center of the matrix. Convolution is utilized to perform picture smoothing. Additionally picture smoothing could be possible with the assistance of average channel which more compelling than convolution when objective is to at the same time decrease the noise in the edges . Average channel replaces a pixel through the average pixel of every last one of neighborhoods.
- ✓ **Gray-Scale Conversion:** The picture gained is in RGB color. It is changed over into gray-scale on the intensity information that it conveys just the vigor data which is not difficult to process as opposed to usage of three parts R(red),G(green),B(blue).

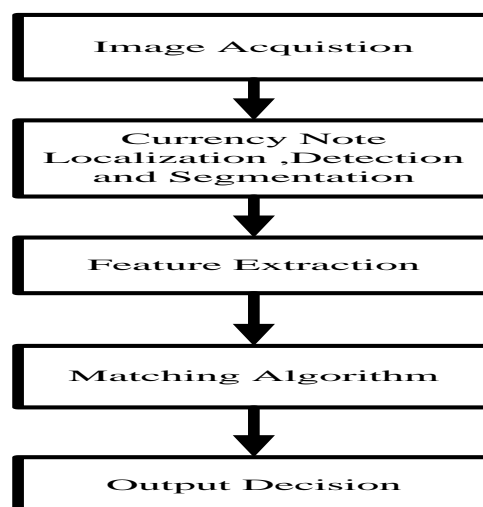


Fig 1: Steps In The Currency Recognition System

Edge detection: edge discovery is a crucial apparatus in picture preparing and machine vision, especially in the ranges of feature detection, extraction, which go for recognizing focuses in a digitized picture at which the picture splendor changes pointedly or, all the more formally, has discontinuities. Edge detection is one of the central steps in image processing, image pattern recognition, image analysis, and machine vision methods.

- ✓ Image segmentation: It divides into objects and regions. The level to which sub division is conveyed relies on upon the issue being illuminated. Division calculation for monochrome pictures by and large are focused around one of the two fundamental properties of intensity values is discontinuity, similarity.
- ✓ Feature Extraction: Feature extraction is the special form to reduce the dimensionality in image processing .It is the strategy for catching the visual substance of pictures for indexing and recovery. At the point when the data information to a calculation is so expansive there is no option be prepared and it is suspected to be famously recurring (much information though very little data) then the information will be changed into a diminished by representation set of the features. In the event that the characteristics concentrated are by the design chosen. It is normal that the properties set will extricate the applicable data from the information to carry out the desired task utilizing decreased representation rather than the full size input Characteristic extraction, includes improving the measure of assets needed to depict the vast set of information.

IV. EVALUATION IN THE ALGORITHMS'

Throughout the years, several algorithms have been anticipated by the various researchers for the consistent currency recognition. In the wake of getting peculiarities of economic standards, it is crucial to perceive the example of the currency on the basis of these features which have to be polished by a compelling successful recognition system called classifier. A standout amongst the most well-known grouping strategies that had been utilized as of late is Artificial Neural Network. A Neural system based recognition scheme was utilized used for The Neural Network comprised of three layers that are input, hidden, output layers. In this system, the picture procured right away was RGB picture and after that it was being changed over into gray scale. Edge detection of the entire gray scale picture was then performed. In the detecting edges, the four attributes of the paper money was edited and segmented. After segmentation, the qualities of the paper cash were extricated. The characteristics of experimental picture are contrasted and the first pre stored picture in the framework. In the event that it matches then the currency is bona fide generally with the counter feit. At that point they discovered the tone and immersion for imputing the picture and assessed the neural system for those characteristics On the off possibility that the tone and immersion limits from the neural system were not exactly the current picture thresholds limit, then the current picture was viewed as bona fide else the picture was announced as a fake one. And the next ,the comparative work is carried were they utilized picture histogram focused around which abundance of distinctive shades in a paper money was computed and contrasted and the one is used as reference for the currency[17]. They additionally utilized Markov affix idea to model surface of the paper currency as the monetary forms as an irregular procedure lastly utilized ensemble neural system (ENN) with negative relationship for alignment. The further work as carried out to give an alternate neural system based on the currency order framework utilizing negatively corresponded Ensemble Neural Network. In the evolution they

concentrated more on the ROI by utilized with Pattern Recognition and Neural Networks matching procedure. The Pattern Recognition and Neural Networks matcher strategy was utilized to match or discover cash value or denomination of paper. The work extended to the Neural Network based classification and these are utilized in the neural system that uses histogram based extraction and multilayer Perception model for order. The feed forward back propagation algorithms of the three layers are introduced for the currency note classification notes. The evolution is carried to increase the effective and less time consuming in the real time applications. And it is started to increase the heuristic characteristics of the contrast and brightness. The estimation of work depends on the extrinsic factors of the sensors several works are carried out in the color images .mainly Indian currency reformation are on the base of color. And further investigation is towards to locate the monetary order utilizing an arrangement of Light Dependent Resistor sensors; and Light Emitting Diode lights which are modified to sense the shade examples of the certified receipts next the further evolution is towards filters like wiener filter is used for the reduction of the drift and at the same time the histogram techniques are used in many currency identification techniques.

V. SOME IMPORTANT TECHNIQUES

5.1 Texture Based Recognition Techniques

Texture is an exceptionally valuable feature for Currency Recognition.. Textural features relating to human visual discernment are extremely helpful for ideal feature determination and surface analyzer plan. There are some situated of composition peculiarities that have been utilized regularly for picture recovery. Tamura characteristics such has directionality, coarseness, contrast, Tamura coarseness is characterized as the normal of coarseness measures at every pixel area inside a composition district. This sort of features can figure specifically from the whole picture without any homogeneity imperative. So the exhibitions of this peculiarity are not acceptable when all is said in done. Therefore, an enhanced variant of this peculiarity by speaking to the coarseness data utilizing a histogram should to be considered. Multi-determination synchronous auto-backward model watchful edge histogram, MRSAR features gives the results that are influential in recognizing distinctive surface examples. The Gabor features use channels to concentrate surface data at various scales and introductions With respect to composition characteristics, there is an examination of the execution of Tamura features, edge histogram, MRSAR, Gabor surface features, and pyramid-organized and tree-organized wavelet change characteristics. Nonetheless, to accomplish such a decent execution from MRSAR, separation focused around a picture subordinate Covariance framework must be utilized, and along these lines, it builds the extent of features and hunt complexity. Then again, the extraction of Gabor feature is much slower than other composition characteristics, which makes its utilization in expansive databases. Hence Tamura features are not tantamount to TWT, PWT, MRSAR, Gabor, characteristics.

5.2 Placement Rule

The previously, there was some trouble in composition investigation because of absence of satisfactory instruments to describe diverse scales of surface viably. There are some composition based methods. Many works are carried to give a strict definition for visual composition is troublesome .Its structure is just credited to

the lifeless examples in which components or primitives are organized by a placement rule. Consequently it can be composed as $f = R(e)$ Where R is indicating a placement rule or connection and e is the element. There is a situated of peculiarities by which all data examples are measured and which give politely dispersed results. For this reason, it is obliged to have both extremes characterizes for each one features. Particularly, coarseness is a very key element in composition. With a specific end goal to enhance alternate features, the results should be well established. As for line-similarity, regregularity, and unpleasantsness, and got significant correspondences in the middle of computational and mental estimations, but more effort is obliged to portray accurately for the texture elements on which it depends on the above mentioned three features.

The Pattern recognition is conclusions focused around earlier learning. A manifestation of this is the characterization of articles focused around a set of pictures. There are number of systems exist in the writing which make utilization of example recognition features to a portion of the great issues. These strategies are extensively centered on Vector quantization based histogram demonstrating. Vector quantization (VQ) is a system for testing a d-dimensional space where each one point, XJ, in a set of information is supplanted by one of L model focuses. The model focuses are picked such that the whole of the separations from every information point, XJ, to its closest model point is minimized. To start with he gathers the information, amid the information accumulation stage different foundation colors, including dark, white, red, and blue, were tried for segment ability. Adobe Photoshop was utilized to focus the RGB estimations of the coin and its experience. At that point a Segmentation system was connected to these pictures. After the information accumulation next step is Coin Segmentation and Cropping. In this step coins were sectioned from their experiences utilizing some adjustment. After completion of division editing system was executed to place the edges of coin. After this Features were extricated from the coins by convolving surface layouts with each one picture, with edge location formats. Next step was preparing, in these Five dimes, nickels, pennies, and quarters were utilized for preparing information.

The color based techniques mainly includes the histogram technique in the image. It is developed by numbering the quantity of pixels of each one color. Histogram depicts the worldwide color circulation in a picture. It is not difficult to register and is uncaring to little changes in the view position. The reckoning of shade histogram simply includes checking the quantity of pixels of determined color. Subsequently in a picture of determination $m \times n$, the time intricacy of registering color histogram is $O(mn)$. It is truly inhumane to little change in VP features is especially wanted in this task as the VP from which the picture of coin note will be procured can change. Color histogram system will suit when the isolation is to be carried out between a scope of shades and an unmistakable shade. This strategy may suit the prerequisites when isolation is to be done among very nearly comparative colors. Shade histograms likewise have a few limits. Color histograms depict which colors are exhibit in the picture and in what amounts; shade histograms give no spatial data. Shade soundness vector is a refined methodology of cognizance histogram. In this approach, the neighborhood properties of pictures are muller over as difference to CH system that is a worldwide one. In this system, areas are based upon the coherency. The color indexing calculation utilizes the back-projection of the two fold shade sets to concentrate shade districts from pictures. This procedure accommodates both the robotized extraction of districts and representation of their color substance. This overcomes the some of the problems such as spatial localization, and indexing and distance computation. as high-dimensional feature vectors etc.

VI. CONCLUSION

New advanced tools and development in the technology shows that the visually impaired individually issues can be hardened in today's reality. In this paper we have surveyed about technologies which are conceptualized on the robustness and the computational for Indian Currency Note Denomination Recognition system especially for visually impaired ones. This paper presents a brief overview about the existing prior techniques and evolutions in the techniques.. The work gives more effective to understand the methods and algorithms involved in the system.

REFERENCES

- [1] Jain, V.K.2013.Indian Currency Denomination Identification Using Image Processing Technique”, Vipin Kumar Jain et al, (IJCSIT) International Journal of Computer Science and Information Technologies. Vol. 4, No.1 ,PP. 126-128
- [2] Mirza, R., and Nanda, V.2012. Paper Currency Verification System Based on Characteristic Extraction Using Image Processing. International Journal of Engineering and Advanced Technology (IJEAT). ISSN: 2249 – 8958. Vol. 1. Iss.3
- [3] Chakraborty, K., Basumatary, J., Dasgupta, D., Kalita, J.C., and Mukherjee, S.2013. Recent Developments in Paper Currency Recognition System. International Journal of Research in Engineering and Technology.Vol. 2, Iss. 11
- [4] Reel, P.S., Krishan, G., and Kotwal, S.2011. Image processing based heuristic analysis for enhanced currency recognition. International Journal of Advancements in Technology, Vol.2, No. 1, pp. 82-89
- [5] Pawade, D., Chaudhari, P., Sonkamble, H.2013. Comparative Study of Different Paper Currency and Coin Currency Recognition Method. International Journal of Computer Applications. Vol. 66,No.23
- [6] Ali, A., and Manzoor, M.2013. Recognition System for Pakistani Paper Currency. Research Journal of Applied Sciences, Engineering and Technology. Vol. 6(16). pp. 3078-3085
- [7] Krishan, G.2010.Image Processing Based Feature Extraction of Indian Currency Notes. PhD diss., Thapar University
- [8] Danti, A., and Nayak, K.2014. Grid Based Feature Extraction for the Recognition of Indian Currency Notes. International Journal of Latest Trends in Engineering and Technology (IJLTET), Vol.4, Iss. 1
- [9] Tanaka, M., Takeda, F., Ohkouchi, K., and Michiyuki, Y.1998. Recognition of paper currencies by hybrid neural network. In Neural Networks Proceedings, IEEE World Congress on Computational Intelligence. The 1998 IEEE International Joint Conference. Vol. 3. pp. 1748-1753
- [10]Malik, S., Bajaj, P., Kaur, M.2014. Sample Coin Recognition System using Artificial Neural Network on Static Image Dataset. International Journal of Advanced Research in Computer Science and Software Engineering. Vol. 4, Iss. 1
- [11]Pathrabe, A. M. T., and Bawane, N. G.2010. Paper Currency Recognition System using Characteristics Extraction and Negatively Correlated NN Ensemble. International Journal of Latest Trends. Vol.1, Iss. 2

- [12] Sannakki, S. S., and Gunjale, P. J. 2014. Recognition and Classification of Currency Notes using Discrete Wavelet Transform. International Journal of Emerging Technology and Advanced Engineering. Vol.4, Iss.7
- [13] Velu, C.M., Vivekanadan, P., and Kashwan, K. R. 2011. Indian Coin Recognition and Sum Counting System of Image Data Mining Using Artificial Neural Networks. International Journal of Advanced Science and Technology, Vol. 31, pp. 67-80, 2011
- [14] Ravi, V., and Ravi, S. 2013. Indian Currency Notes Recognition Using Principle Component Analysis Based On Local Binary Pattern. International Journal of Review in Electronics & Communication Engineering, Vol. 1, Iss. 2
- [15] Bhavani, R., and Karthikeyan, A. 2014. A Novel Method for Banknote Recognition System. International Journal of Innovative Research in Science, Engineering and Technology, Vol. 3, Iss.1
- [16] Sargano, A. B., Sarfraz, M., Haq, N.U. 2013. Robust Features and Paper Currency Recognition System. ICIT ,The 6th International Conference on Information Technology
- [17] Aggarwal, H., and Kumar, P. 2012. Indian Currency Note Denomination Recognition in Color Images. International Journal on Advanced Computer Engineering and Communication Technology. Vol.1, Iss.1, ISSN. 2278 – 5140

STUDIES ON MICROSTRUCTURE AND MECHANICAL PROPERTIES OF MODIFIED LM25 ALUMINIUM ALLOY

Venkatachalam G¹, Kumaravel A², Arun Kumar N³,
Dhanasekaran Rajagopal⁴

^{1,2,4} Department of Mechanical Engineering,

K. S. Rangasamy College of Technology, Tiruchengode (India)

³ PG Scholar, Department of Mechanical Engineering,

K. S. Rangasamy College of Technology, Tiruchengode (India)

ABSTRACT

In the present investigation, aluminium alloy LM25 grade is chosen as matrix material with zirconium particles as reinforcement. Modified LM25 alloys are fabricated by stir casting process. Chemical compositions, Rockwell hardness and tensile testing are performed to find the mechanical properties for fabricated modified LM25 alloy. The results revealed that the hardness value increases and the tensile value decreases with Zr addition. Microstructures of the samples were investigated using the optical microscope.

Keywords: Aluminium alloy, LM25, Hardness, Microstructure, Tensile property

I. INTRODUCTION

For the last few decades, the development of materials shifted from monolithic alloy to composite materials to meet the global industrial needs. The properties of composites are strongly dependent on the properties of their constituent materials, their distribution and the interaction among them. The reinforcements are in the form of flakes, particulates and fibers. Reinforcement enhances the strength, hardness, stiffness, wear resistance, friction coefficient, thermal conductivity and temperature resistance capacity and lowers the density of MMC.

Al-Si-Mg casting alloys are increasingly used in the automotive and aerospace industries for critical structure applications due to their excellent casting ability, weldability and corrosion resistance, and particularly good tensile and fatigue properties [1]. A356 alloys naturally have an elastic modulus of about 70 GPa, which is about one-third of the elastic modulus of the majority kinds of steel and steel alloys [2]. The yield strength and hardness of these alloys are usually improved by solution treatment and artificial aging through the formation of fine Mg₂Si precipitates [3,4]. However, the strength of these alloys degrades quickly above working temperatures of 130–150 °C because of rapid coarsening of the precipitates. To improve the mechanical properties and thermal stability of Al-based alloys, dispersoid-forming elements such as Zr, Mn and Cr can be added to the alloy. Of these elements [5-7], Zr provides on the one hand an increase of the strength at room temperature and on the other, microstructural stability at higher temperatures by forming very fine stable dispersoids. In the Al-Zr binary

system, an ordered Al_3Zr trialuminide may be precipitated from a super saturated solid solution during post-solidification aging [6-8]. The hardness of the Zr-containing alloys did increase by an average of 8% and 15% after solution treatment for 8 h and 24 h, respectively. The addition of Zr to the alloy had a grain refining effect on the structure and reduced the average grain size to 0.7 μm [9]. In the present work, the effect of addition of small amount of lithium and zirconium on microstructure, hardness and tensile property of modified LM25 alloy has been investigated.

II. EXPERIMENTAL WORK

Table 1 Composition of aluminium alloy (LM25)

Elements	Cu	Si	Mg	Mn	Fe	Ni	Zn	Ti	Pb	Sn	Al
Wt. %	0.07	3.15	0.5	0.17	0.9	0.01	0.04	0.02	0.03	0.002	Balance

The constituent elements of LM25 alloy are presented in Table 1. A weighted quantity of the LM25 Al alloy was melted in clay bonded graphite of 2 Kg capacity using a small electrical furnace. The experimental setup is shown in Fig. 1. The melt was maintained at about 750°C and stirred using a mild steel impeller at a speed of 600 RPM to create the vortex. The reinforcement material, zirconium particles of 100 to $240\mu\text{m}$ of size were added and the stirring process was continued for 10 to 15 minutes and then the composite slurry was poured into the mild steel die, which was preheated to about 300°C .

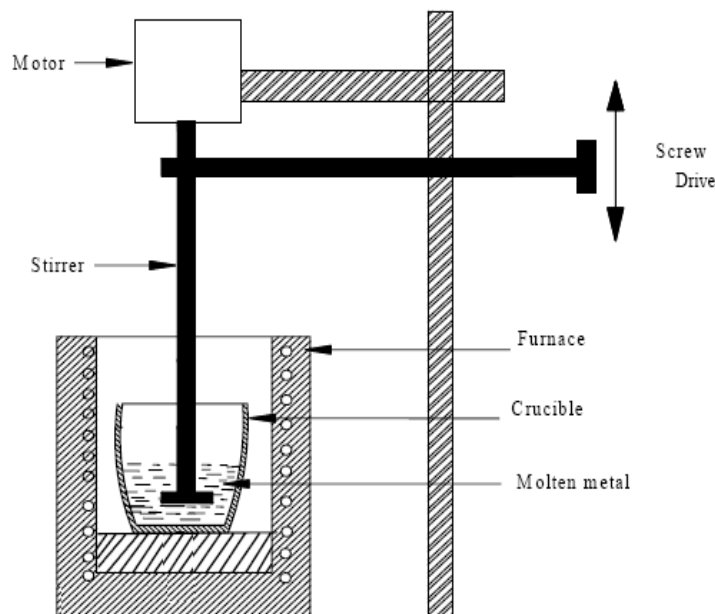


Figure 1 Mechanical stir casting setup and stirring process

Microstructures of the modified LM25 alloy were analyzed to verify the reinforcement distribution on composites. The tensile test specimens were made according to ASTM: E8M-13a standard as shown in Fig. 2. Tensile tests were carried out in a computerized testing machine at a strain rate of 1 mm/min. Rockwell hardness test is performed on the samples using digital Rockwell hardness testing machine.

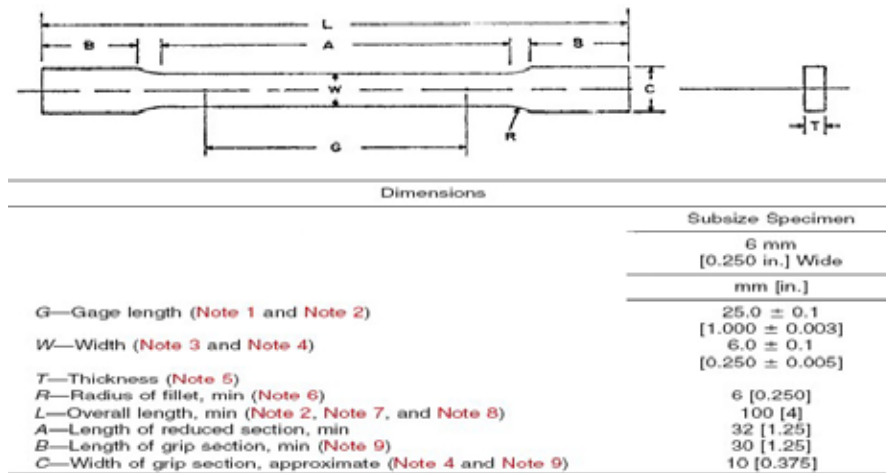
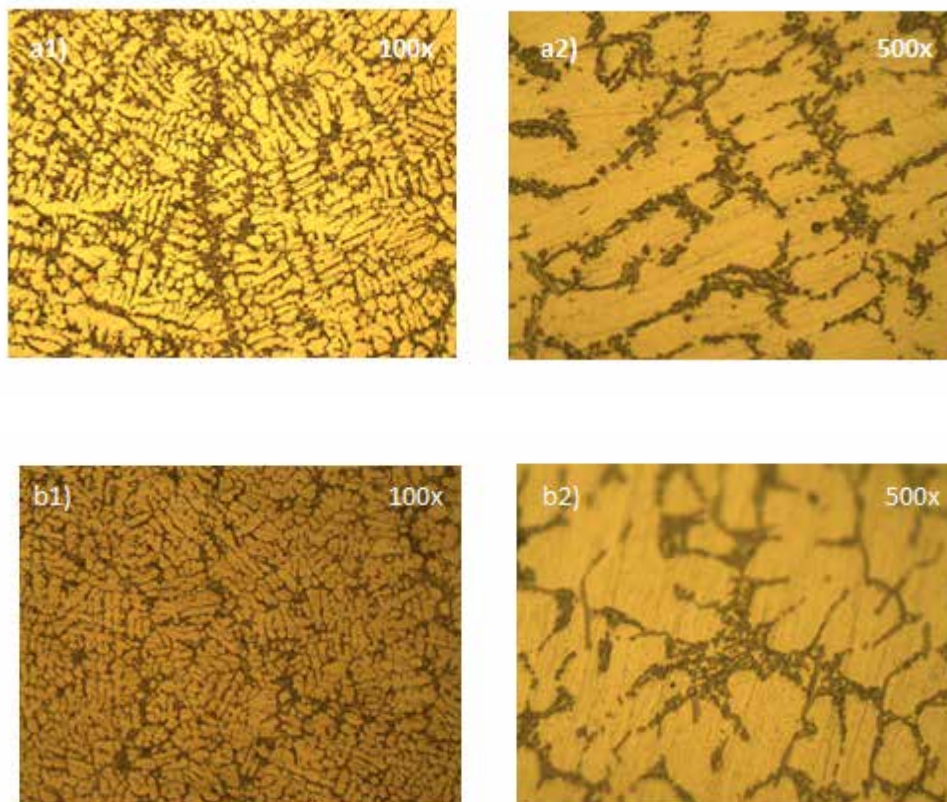


Figure 2 Size of tensile Specimen

III. RESULTS AND DISCUSSION

3.1. Microstructure

Microstructural examination of the modified LM25 alloy was carried out to confirm the dispersion of Zr particles. Cross sectional of the samples revealed the presence of inter-dendritic network of eutectic silicon, Zirconium particles (mostly rounded, less angular) and Mg₂Si particles distributed in a matrix of aluminum solid solution throughout structure as shown in Fig. 3.



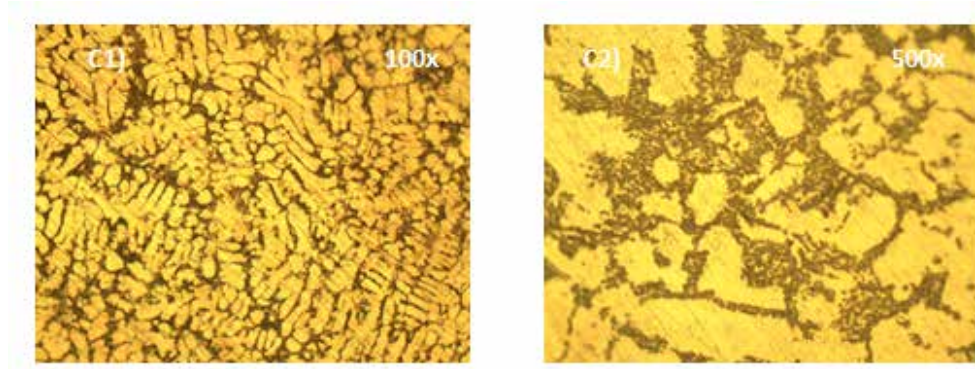


**Figure 3 Microstructures of the modified LM25 alloys,
(a) 0.25 wt% Zr, (b) 0.5 wt% Zr and (c) Zr-free**

3.2. Hardness

The results of hardness tests are shown in Table 2. It can be seen that the initial hardness of the unmodified alloy was 60HRB that decreased to 48 HRB and increases with the addition of Zr. According to the micro structural modification so β inter metallic, hardness should increase with the addition of Zr, but the results indicate that hardness obviously declines initially. Because of porosity in the composites the hardness value is decreased and the hardness is very sensitive to the porosity volume fraction. The hardness of the fabricated composite can be enhanced by age hardening process.

Table 2 Rockwell hardness of modified LM25 alloy

Sample No.	Composition of samples	Hardness value (HRB)
1	Al + 0%Zr	60
2	Al + 0.75%Zr	48
3	Al + 1.00%Zr	53

3.3. Tensile Property

The average ultimate tensile strength (UTS) and elongation values of composites with and without Zr are illustrated in Table 3. It is evident that the addition of Zr decreases the tensile property. UTS is decreased from 230 to 165MPa and elongation percentage is reduced from 6% to 3.8%. Further increase of Zr decreases the tensile property. The tensile properties of composites can be increased with the age hardening process.

Table 3 Ultimate tensile strength and elongation of modified LM25 alloy

Sample No.	Composition of samples	UTS (Mpa)	Elongation (%)
1	Al + 0%Zr	230	6.0
2	Al + 0.75%Zr	165	3.7

3	Al + 1.00%Zr	162	3.9
---	--------------	-----	-----

IV. CONCLUSION

The effect of Zr and Li on the microstructure and mechanical properties of modified LM25 alloys were investigated. The following conclusions were drawn:

1. Presence of less porosity is confirmed with the microstructure analysis.
2. Addition of Zr to the LM25 alloy decreased the hardness values initially and then increases with the rise of Zr. Further the hardness of the modified LM25 alloy can be enhanced with age hardening process.
3. The ultimate tensile strength and elongation percentage of the modified LM25 alloy decreases with the addition of Zr.

REFERENCES

- [1] B. Dang, Y.B. Li, F. Liu, Q. Zuo and M.C. Liu, Effect of T4 heat treatment on microstructure and hardness of A356 alloy refined by Ga + In + Sn mixed alloy, *Materials and Design*, 57, 2014, 73–78.
- [2] ShashiPrakashDwivedi, Satpal Sharma and Raghvendra Kumar Mishra, A356 Aluminum Alloy and applications- A Review, *Advanced Materials Manufacturing & Characterization*, 4(2), 2014.
- [3] N.A. Belov, D.G. Eskin and A.A. Aksenov, *Multicomponent phase diagrams: applications for commercial aluminum alloys*, Elsevier Science, 2005.
- [4] P. Sepehrband, R. Mahmudi and F. Khomamizadeh, Effect of Zr addition on the aging behavior of A319 casting alloy, *Scr Mater*, 52, 2005, 253–257.
- [5] R. Mahmudi, P. Sepehrband and H.M. Ghasemi, Improved properties of A319 casting alloy modified with Zr, *Mater Lett*, 60, 2006, 2606–2610.
- [6] K.E. Knipling, D.C. Dunand, and D.N. Seidman, Nucleation and precipitation strengthening in dilute Al–Ti and Al–Zr alloys, *Miner Met Mater Soc ASM International*, 38A, 2007, 2552–2563.
- [7] J.Q. Guo and K. Ohtera, An intermediate phase appearing in L12–Al₃Zr to DO23–Al₃Zr phase transformation of rapidly solidified Al–Zr alloys, *Mater Lett*, 27, 1996, 343–347.
- [8] A.A. Gokhale and V. Sinagh, Effect of Zr content and mechanical working on the structure and tensile properties of AA8090 alloy plates, *J Mater Proc Technol*, 159, 2005, 369–376.
- [9] B. Baradarani and R. Raiszadeh, Precipitation hardening of cast Zr-containing A356 aluminium alloy, *Materials and Design*, 32, 2011, 935–940.

PCB DETECTION AND CLASSIFICATION USING DIGITAL IMAGEPROCESSING

¹ Shashikumar Vishwakarma, ² SahilTikke, ³Chinmay Manurkar,
⁴Ankit Thanekar

^{1,2,3,4} Electronics and Telecommunication (B.E), KJSIEIT, (India)

ABSTRACT

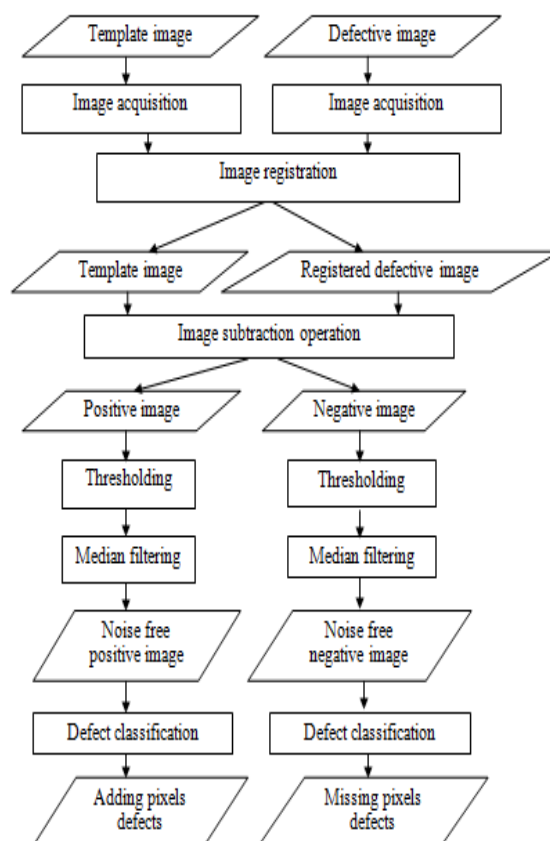
A Printed Circuit Board defect detection and classification system uses machine vision. Machine Vision helps counter difficulties that occur in manual inspection. It eliminates the subjective aspects and provides fast, quantitative, and dimensional assessment. Defects present in PCBs are short circuit, open circuit, pin hole, under-etch, mouse-bite and missing hole. These defects are classified using Image Processing techniques. The PCB inspection process is then improved using geometrical image registration so that any image which is different with the reference image can be aligned. This helps in accurate image processing results. Minimum Threshold technique is used to set a threshold level for the respective image and median filtering is used to solve the uneven illumination problem.

I INTRODUCTION

Bare PCB is a PCB without any placement of electronic components which is used along with other components to produce electronic goods. In order to reduce cost spending in manufacturing caused by the defected bare PCB, the bare PCB must be inspected. Image subtraction must be used to detect defects on the PCBs. However, image subtraction operation that has been utilized to detect defects between defective and template images cannot be used directly as it contributes unwanted noise due to misalignment and uneven binarization and thus, the accuracy of the defect detection could be decreased. Since the nature of real PCB images is different compared to computer generated PCB images, an image registration must be employed at first in order to get well-aligned defective image against template image. Then, all pixels in the template image are subtracted against the registered defective image to get two output images known as positive and negative images. Next, by applying image thresholding and filtering techniques, noise free positive and negative images are produced. Starting from here, the two images can be used as for the defect classification. Moganti et al. proposed three categories of PCB inspection algorithms: Referential approaches, Non Referential approaches and Hybrid approaches. Referential approaches consist of image comparison and model-based technique. Non-referential approaches or design-rule verification methods are based on the verification of the general design rules that is essentially the verification of the widths of conductors and insulators. Lastly, hybrid approaches involve a combination both of the referential and the non-referential approaches. These PCB inspection approaches mainly concentrated on defects detection. However, defects detection did not providesatisfactory information for repairing and quality control work, since the type of detected defects cannot be clearly identified. Based on this incapability of defects detection, defect

classification operation is needed in PCB inspection. Therefore, an accurate defect classification procedure is essential especially for an on line inspection system during PCB production process. In literature, Wu et al., Rudi Heriansyah and Abu-Bakar (2004), Rau and Wu (2005), and Ibrahim et al. (2011) have proposed PCB inspection systems in classifying defects. In this project, a new PCB inspection system on PCB images has been proposed by adapting similar algorithm that comes from Ibrahim et al., (2011).

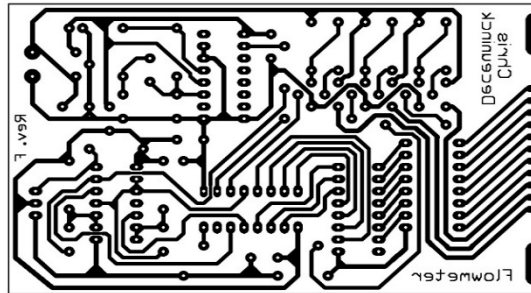
II METHODOLOGY



Some of the defects in PCB are short circuit, open circuit, pin hole, under-etch, mouse-bite and missing hole. In all these defects Open and short circuit are fatal defects while others fall under potential defects category. Assuming image has been registered. PCB images are available in computer database which are acquired from a camera device. After this we perform image complement. In image complement operation we take negative of the test image for further operations. After this we can use image subtraction to obtain the result. Image subtraction is an operation used to compare every pixel value and according to that difference is calculated. These differences are then compared to and presented in the form of equations. It is used after image registration. Images that we get from image subtraction are in positive and negative format. To convert those images in binary form we take threshold of the image. We use minimum threshold technique. In this technique a minimum threshold value is calculated and put as threshold. The value obtained in our case is 156. After getting result we need to classify them. Defects are classified using several operations like arithmetic and morphological operations. Following are the defects which are classified, defects in PCB are short circuit, open circuit, pin hole, under-etch, mouse-bite and missing hole.

III. RESULTS

Performing the following operations we can detect and classify the defects.



3.1 Hole Defect

Hole defect is one of the defects in which extra holes etched. Due to this the circuit malfunctions. To detect this defect we use image subtraction and subtract the template image and the obtained image to spot the difference and correct it. Below is the result obtained after subtracting the image.

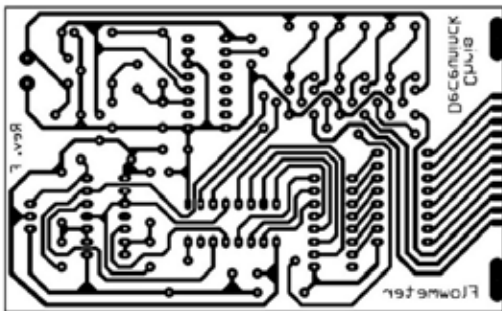
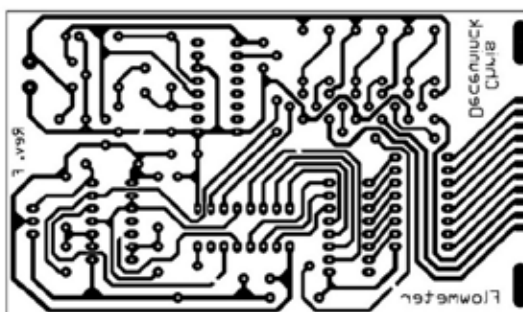


Image with defects

3.2 Open Circuit Defect

Open circuit defect is one of the fatal defects. In this some of the circuit lines don't get etched properly and there are cuts in the circuit due to which circuit is not complete. Same procedure as above is used to detect the defect. Reference image is subtracted from the negative of the defective PCB image. Hence the defect is detected.

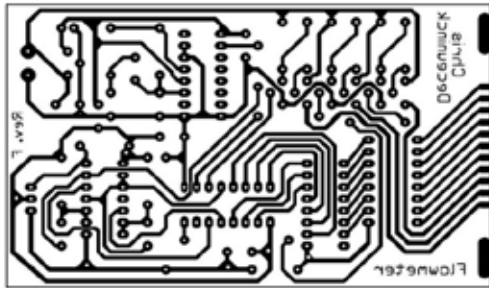


Open Circuit Defect

Detected Defect

3.3 Missing Pin Holes

In Missing Hole defect, the PCB contains some missing holes. These holes are crucial because they are to be used to connect resistors, capacitors etc. But since the holes are missing we cannot use them. Hence to detect this defect early we can use a template image for reference and another image of the defective PCB. We use image subtraction and get the following result that is shown below.



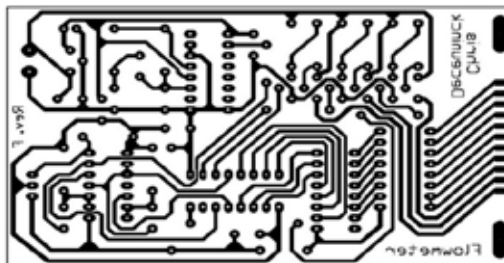
Missing pin hole defect



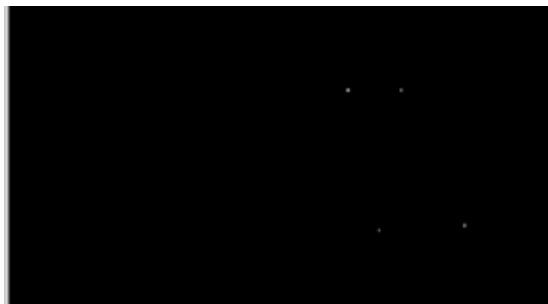
Detected Defects

3.4 Short Circuit Result

This is the second fatal defect after open circuit defect. In this defect when the PCB circuit lines are not spaced equally then the circuit lines get overlapped due to which the circuit gets short circuited. Same procedure as above is used to detect the defects. Below is the result obtained after using image subtraction procedure.



Short Circuit Defect



Detected Defect

IV CONCLUSION

Hence by using median filtering , image complement , image subtraction and by assuming images are registered successfully detected and classified the following defects ,WZ short circuit, open circuit, pin hole, under-etch, mouse-bite and missing hole in PCB using Digital Image Processing.

REFERENCES

- [1] A printed circuit board inspection system with defect classification capability, Ismail Ibrahim, Syed Abdul

Rahman, Syed Abu Bakar, Musa Mohd. Mokji, Jameel Abdulla Ahmed Mukred, Zulkifli Md.

Yusof, Zuwairie Ibrahim, Kamal Khalil, Mohd Saberi Mohamad, faculty of Electrical Engineering, faculty of Computer Science and Information system, University Teknologi Malaysia Johor, 81310, Malaysia.

Survey, Computer Vision and Image Understanding, vol.63, no.2, pp.287-313.

- [2] H. Rau and C.H. Wu (2005), Automatic optical inspection for detecting defects on printed circuit board inner layers, International Journal of Advanced Manufacturing Technology, vol.25, no.9-10, and pp.940-946. S. Periaswamy and H. Farid (2006), Medical image registration with partial data, Medical Image Analysis Journal, vol.10, no.3, pp.452-464.
- [3] Ibrahim et al., (2011). International Journal of Innovative Management, Information & Production ISME International ©2011 ISSN 2185-5439 Volume 3, Number 1, March 2011
- [4] Google Image Search: www.google.com/Images S Jayaraman, S Esakkirajan and T Veerakumar, Digital Image Processing, Tata MCgraw-Hill.

HEATING OF EN9 STEEL BY USING MICROWAVE ENERGY AND COMPARING WITH CONVENTIONAL HEATING TECHNIQUE WITH THE HELP OF MICROSTRUCTURE

Shital Patil¹, Suraj Shinde², Vasim Shaikh³, Yogesh Kamble⁴.

¹B.E.(Mechanical) Engineer, Manugraph India Pvt. Ltd. Kolhapur, Maharashtra, (India)

²Asst.Engineer, Renuka Sugars Pvt. Ltd, Belgaum, Karnataka, (India)

³Lecturer, Sharad Institute of Technology, Polytechnic, Yadrav-Ichalkaranji, Maharashtra, (India)

⁴Asst.Professor, Dhananjay Mahadik Group of Institutions, Vikaswadi Kagal, Maharashtra (India)

ABSTRACT

The microwave heating technology began with heating food and later on extending applications to the processing of a wide variety of materials, like ceramics, polymers and composites; now offers wide applications in the area of metallic material processing too. The microwave processing of materials is a relatively new technology that provides new approaches to improve the physical properties of materials; provides alternatives for processing materials that are hard to process; reduces the environmental impact of materials processing. The growing interest is partly the result of increased awareness among scientists, processing engineers, and potential users about the benefits of microwave processing. Microwaves for metallic material processing are a challenging area of research owing to reflection of electromagnetic waves by most of the metals at ordinary conditions.

Keywords: Volumetric Heating, Electromagnetic Spectrum, Potential Heating Mechanism, Microwaves.

I. INTRODUCTION

The spectrum of electromagnetic waves spans the range from a few cycles per second in the radio band to 10^{20} cycles per second for gamma rays. Microwaves occupy the part of the spectrum from 300 MHz (3×10^6 cycles/s) to 300 GHz (3×10^{12} cycles/s). Within this portion of the electromagnetic spectrum there are frequencies that are used for cellular phones, radar, and television satellite communications. For microwave heating, two frequencies, reserved by the Federal Communications Commission (FCC) for industrial, scientific, and medical (ISM) purposes are commonly used. The two most commonly used frequencies are 0.915 and 2.45 GHz. Recently, microwave furnaces that allow processing at variable frequencies from 0.9 to 18 GHz have been developed for material processing. [1] Originally, microwaves were principally used for communication. In 1950, the use of microwave energy to heat materials was discovered. Now microwave ovens have become common for heating food products in the home. The potential advantages of microwave heating have led researchers to design and implement new processes for industrial use. Although some non-thermal microwave effects have been observed and claimed by researchers, the main application of microwave processing of

materials is in heating. The most prominent characteristic of microwave heating is volumetric heating, which is quite different from conventional heating where the heat must diffuse in from the surface of the material. Volumetric heating means that materials can absorb microwave energy directly and internally and convert it to heat. It is this characteristic that leads to advantages using microwaves to process materials. Beginning in the late 1980s, there was growing interest in high temperature microwave processing of materials. With some successful applications at laboratory scale, for example, sintering of ceramics, microwaves are justified as a potential heating mechanism to replace some conventional heating methods [2].

Melting metals in traditional furnaces such as cupola furnace, blast furnace, crucible furnace etc. consumes significant amount of energy along with possibilities of material and energy losses and some safety risks. In order to overcome the inherent disadvantages of conventional melting, one or more of the advanced melting technologies such as electron beam melting, infra red melting, plasma melting, microwave melting, solar melting etc. are preferred according to the specific requirements and applications. Microwave heating receives considerable attention due to its major advantages such as high heating rates, reduced processing time, low power consumption and less environmental hazards. During microwave heating, large amount of heat may be generated for a lossy material throughout the volume, whereas for conventional heating, the material is heated via an external heat source and subsequent radiative transfer [3].

In recent years, microwave processing of metal/alloy powders have gained considerable potential in the field of material synthesis. Microwave heating is recognized for its various advantages such as: time and energy saving, rapid heating rates, considerably reduced processing cycle time and temperature, fine microstructures and improved mechanical properties, better product performance, etc. Microwave material interactions for materials having bound charge are well established, but for highly conductive materials like metals, there is not much information available to interpret the mechanism of microwave heating and subsequent sintering of metallic materials. In heating how the thermal profile of electrically conductive powder metal like copper changes with particle size and also with porosity content; in other words, initial green density when the material is exposed to 2.45 GHz microwave radiation in a multimode microwave furnace [4].

Microwave hybrid heating is the most important example of mixed-absorbed heating that is used to sinter material which has low dielectric loss at low temperature and high dielectric loss at high temperature. The microwaves are absorbed by the component that has high dielectric loss while passing through the low-loss material with little drop in energy [5-6]. This can be performed by using material, which is called susceptor, and has high dielectric loss at low temperatures around the green part. At low temperatures, susceptor material absorbs microwave and reaches high temperatures. Then, it can transfer heat to the sample via conventional heating mechanisms. Thus, the sample which has high dielectric loss at high temperatures will be able to absorb microwaves per seconds. A combined action of microwaves and microwave-coupled external heating source (microwave hybrid heating) can be utilized to realize rapid sintering from both inside and outside of the powder compact [7]. The hybrid heating system will heat the sample more readily at low temperatures and at high temperatures will flatten out the temperature profile inside the sample

II. EXPERIMENTATION

Two trials were carried out in a 1050 W domestic microwave oven which was modified later with glass wool insulation to reduce heat loss. This oven was then fixed with a thermocouple along with PID controller. Also

two trials were conducted in muffle furnace of 3500W capacity for conventional heating. Metallurgical heating of EN9 steel in bulk form has been achieved in this work. Suitable susceptor was used for initial coupling of microwaves with metallic materials in MW heating. Bulk pieces were exposed to microwave radiation for 14 minutes in a multimode applicator and 136 minutes in muffle furnace. Photograph of red zone inside the insulation box of microwave oven and muffle furnace as shown in Figures 1.1 and 1.2 respectively.

Specification of microwave oven is given in Table 1.1. Tables 1.2 and 1.3 give the properties of EN 9 steel. Table 1.4 shows the specifications of the muffle furnace used. Samples were heated at 875°C, and soaking time of 20 minutes was maintained. After heating, the specimens were removed from both the furnaces and were subjected to air cooling, oil quenching and water quenching respectively.



Figure 1.1 : Photograph of Red zone inside the insulation box



Figure 1.2 : Photograph of Red zone in Muffle furnace at 875°C

Table 1.1: Microwave oven specification

Model number	KJ17Gww2-mmz
Product	Grill microwave oven
Capacity	17 Litres
Power output (MW)	700 Watt
Power input (MW)	1050 Watt
Power input (Grill)	1000 Watt
Dimensions (cm)	44 x34x25.8
Weight	10.5 kg

Table1.2: Chemical composition of EN9 steel

Carbon	Silicon	Manganese	Sulphur	Phosphorous
0.50%	0.25%	0.70%	0.05%	0.05%

Table1.3: Physical Properties of EN9steel

Density kg/m ³	Coefficient of Thermal Expansion Per °C from 20°C	Modulus of Elasticity N/mm ²
7800	11.6x10-6	206000

Table 1. 4: Muffle Furnace specification

Manufacturer	Biotechniques India
Sl. No.	148
Volt (V)	230
Watts(W)	3500
Model	BTI

III. RESULTS AND DISCUSSION.

After experimentation we got the following results in terms of microstructure. They are illustrated in the following figures. Figure 2.1 shows the microstructure of the sample before heating, which reveals ASTM Grain size 7 to 8 and the appearance of elongated & equiaxed grains with 55 to 45% ferrite.

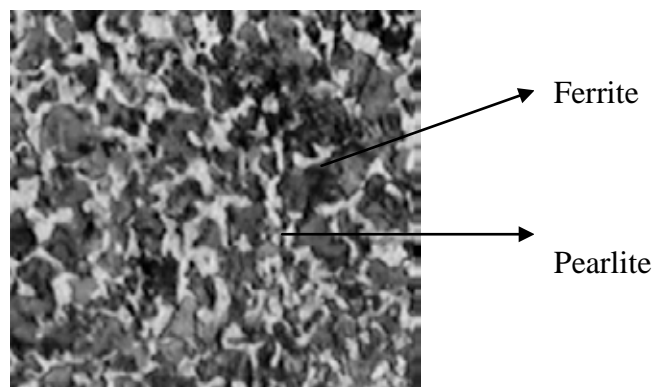


Figure 2.1: Micrograph of original specimen at 250X

Figure 2.2(a) shows the microstructure of an oil quenched specimen (Trial 1) of a muffle furnace, having a coarse structure of martensite. Figure 2.2 (b) shows the microstructure of an oil quenched specimen of microwave heating, having a fine bainite structure which gives better machinability properties. Widmanstätten platelets of ferrite at prior austenite grain boundaries and within grains in a matrix of martensite are shown in Figure 2.2(b).

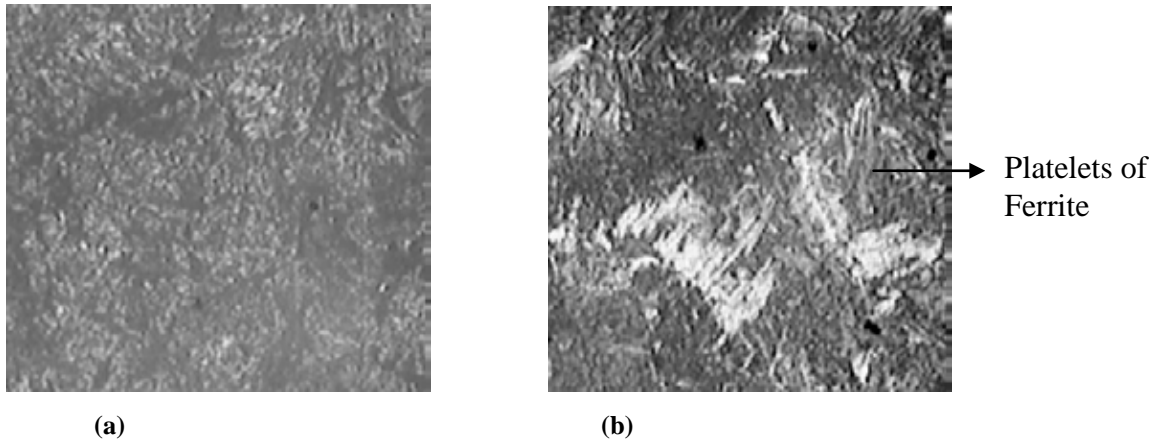


Figure 2.2: Micrograph of oil quenched specimen at 250X. (a) MF Heating, (b) MW Heating.

Figure 2.3(a) shows microstructure of the water quenching specimen(Trial 1) of muffle furnace, martensitic structure is observed. Figure 2.3 (b) shows microstructure of the water quenched specimen of microwave heating, coarse structure has been observed. Specimen has fine structure, along with high toughness. Hardness value increased in MW heating.

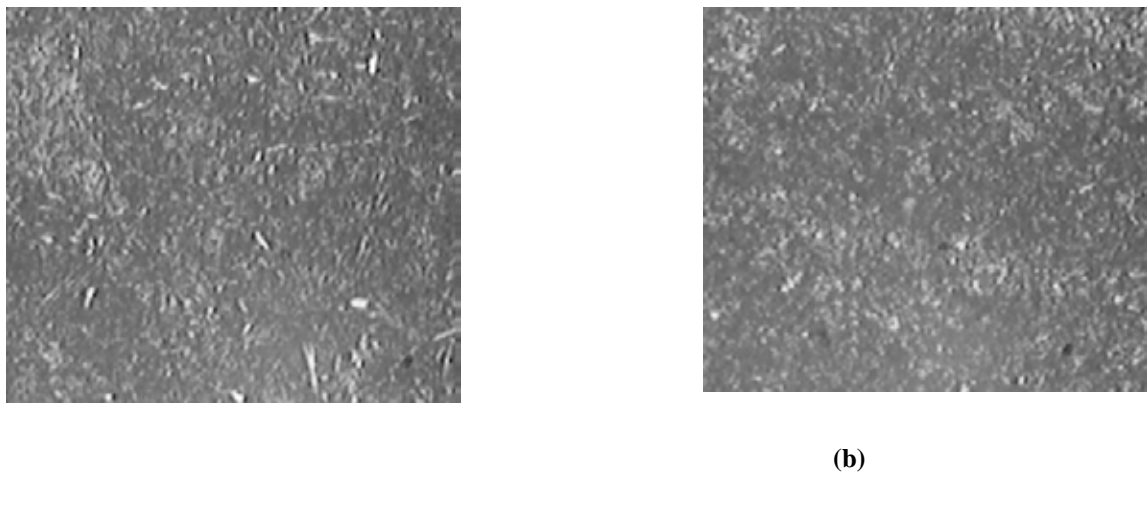


Figure 2.3: Micrograph of water quenched specimen at 250X. (a) MF Heating, (b) MW Heating.

Figure 2.4(a) shows microstructure of the muffle furnace, air cooled (Trial 1) specimen, ASTM Grain size 7 to 8 elongated & equiaxed. Grains predominantly pearlitic matrix with grain boundary ferrite is observed. Air cooling requires maximum time and therefore grain size reduces. Figure 2.4(b) shows microstructure of the air cooled specimen of microwave heating, Widmanstatten platelets of ferrite at prior austenite grain boundary & within grain in a matrix of martensite. From above microstructure coarse structure obtained also machinability has been improved.

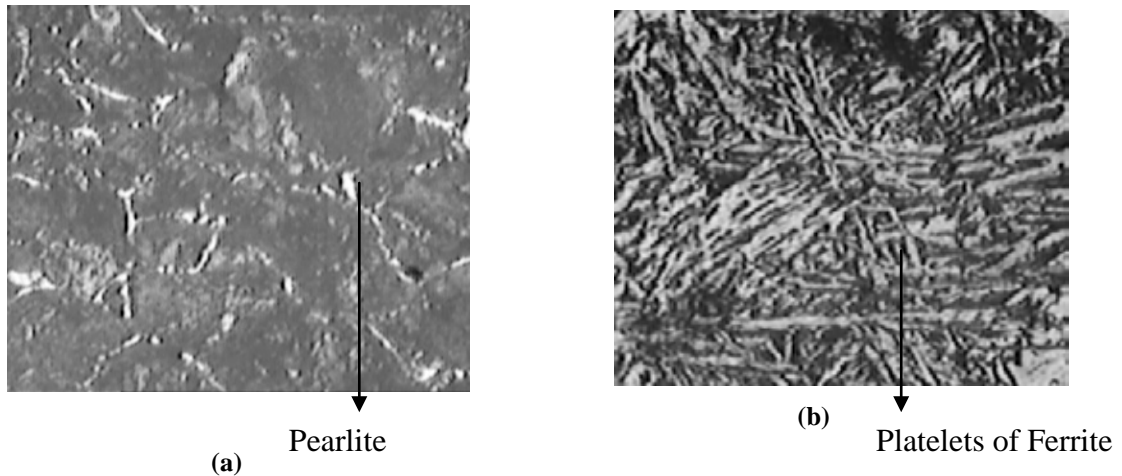


Figure 2.4: Micrograph of air cooled specimen at 250X. (a) MF Heating, (b) MW Heating.

Figure 2.5 (a) shows the microstructure of oil quenched specimen (Trial 2) of muffle furnace having coarse structure of martensite and Figure 2.5(b) shows microstructure of oil quenched specimen of microwave heating having fine bainite structure which gives better machinability properties. Widmanstatten platelets of ferrite at prior austenite grain boundary and within grain in a matrix of martensite in Figure 2.5 (b)

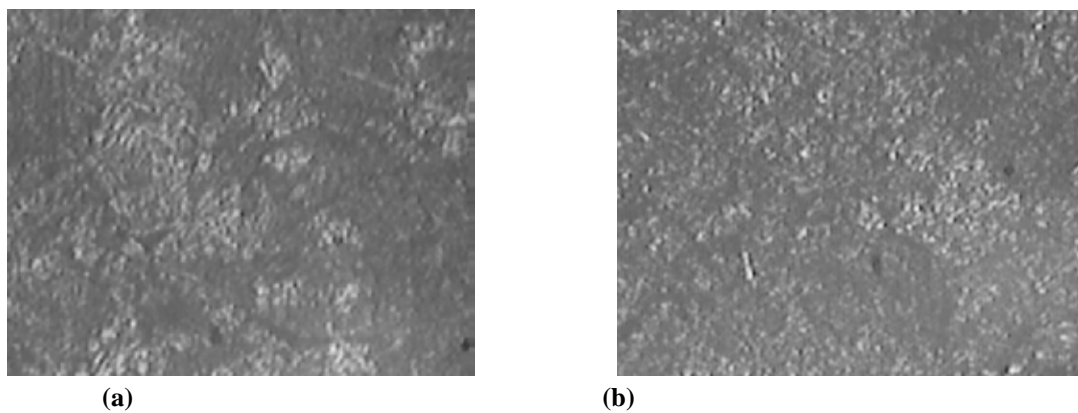


Figure 2.5 : Micrograph of oil quenched specimen at 250X. (a) MF Heating, (b) MW Heating.

Figure 2.6 (a) shows microstructure of the water quenching specimen (Trial 2) of muffle furnace, martensitic structure is observed, coarse structure is seen. Figure 4.6 (b) shows microstructure of the water quenching specimen of microwave heating, which shows >95 % martensite with fine structure and high toughness. Hardness value increased in MW heating.

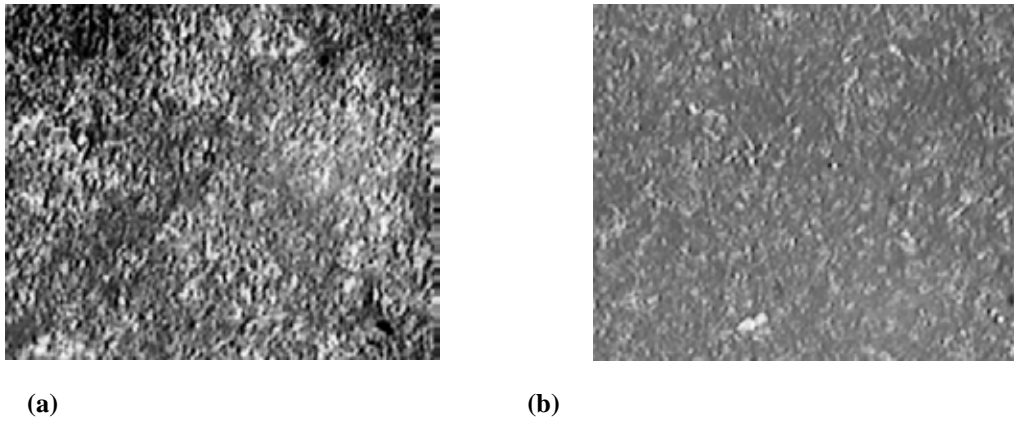


Figure 2.6: Micrograph of water quenched specimen at 250X. (a) MF Heating, (b) MW Heating.

Figure 2.7(a) shows microstructure of the muffle furnace, air cooled specimen, Martensite with grain boundary ferrite is observed. ASTM Grain size 7 to 8 Elongated & Equiaxed. Grains Predominantly pearlitic matrix with grain boundary ferrite is observed. Air cooling require maximum time that's why grain size reduces. Figure 2.7 (b) shows microstructure of their cooled specimen of microwave heating, Widmanstatten platelets of ferrite at prior austenite grain boundary & within grain in a matrix of martensite. From above microstructure coarse structure obtained also machinability has been improve

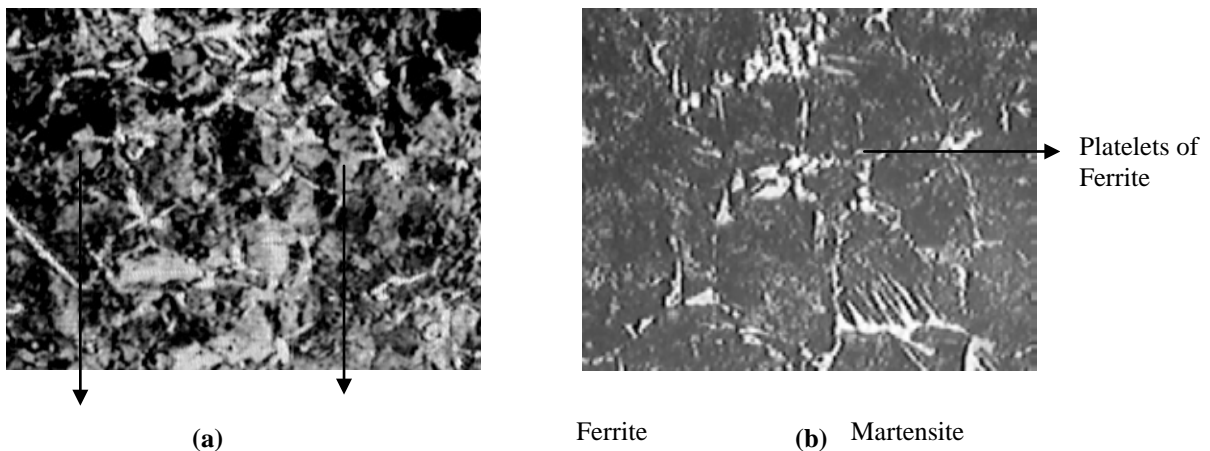


Figure 2.7: Micrograph of water quenched specimen at 250X. (a) MF Heating, (b) MW Heating.

IV. CONCLUSION

In experimentation we have taken various heat treatment processes. From that experimentation we concluded that results of microstructure getting from microwave heating technique are far better than conventional heating technique.

V. ACKNOWLEDGEMENT

Corresponding work has been performed under guidance of Professor Mr.R. I. Badiger and Department of Mechanical Engineering Sharad Institute of Technology College of Engineering Yadrav- Ichalkaranji.

REFERENCES

- [1]EBook: “Microwave Processing Of Materials Committee On Microwave Processing Of Materials”: An Emerging Industrial Technology National Materials, Advisory Board Commission on Engineering And Technical Systems National Research Council.
- [2]Xiaofeng Wu, M.S. “Experimental And Theoretical Study of Microwave Heating Of Thermal RunawayMaterials”, December 2002.
- [3] S. Chandrasekaran, TanmayBasak, S. Ramanathan , “Experimental and theoretical investigation on microwave melting of metals”, Journal of Materials Processing Technology211 (2011).
- [4]AvijitMondal, Dinesh AgrawalandAnishUpadhyaya “Microwave Heating of Pure Copper Powder with Varying Particle Size and Porosity(2008)
- [5]Clark D.E., Sutton W.H. and Lewis,D. “Microwave processing of materials”
Annu.Rev.Mater.sci.,1996,26,299-301.
- [6] M.S. Srinath, Apurbba Kumar Sharma, Pradeep Kumar, “Investigation on Microstructural And Mechanical Properties of Microwave Processed Dissimilar Joints”, Journal of Manufacturing Processes 13 (2011) 141–146.

SURVEY ON: IMAGE SEGMENTATION USING REGION BASED ALGORITHMS

Pranali Parvekar¹, Rachna Dhannawat²

¹M.Tech Student , ²Assistant Professor

U.M.I.T, S.N.D.T University SANTACRUZ (W)

ABSTRACT

The goal of image segmentation is to partition an image into certain number of pieces that have coherent features and to group the meaningful pieces together. Human interactions involved in segmentation should be as less as possible hence to overcome with the disadvantages of image segmentation some techniques were developed which will provide better result of image segmentation. We compared some papers out of which fast interactive image segmentation to locate multiple similar colored objects is found better than other methods.

Key Words: *L0 Smoothing Filter*

I. INTRODUCTION

Images are considered as one of the most important medium of conveying information, in the field of computer vision by understanding images the information extracted from them can be used for other task for example navigation of robots, finding injurious tissues from body scans, detection of cancerous cells, and identification of an airport from remote sensing data. Hence their is strong need of methods which will provide to extract information from the images. Image segmentation is the process of separating or grouping an image into different parts. These parts normally correspond to something that humans can easily separate and view as individual objects. Computers have no means of intelligently recognizing objects, and so many different methods have been developed in order to segment the image. The segmentation method process is based on various features found in image. This might be Color information that is used to create histogram, or information about the pixels that indicate edges or boundaries or texture information thus image segmentation is first step in image analysis. there are different types of image segmentation such as compression based, histogram based, region based and cluster based methods. In compression based here The segmentation tries to find the pattern in an image and any regularity in the image can be used to compress the values in order to get well defined image. Histogram based methods are very efficient compared to other image segmentation methods because in this techniques histogram is computed from all the pixels in an image and the peaks and Valley in the histogram are used to locate the cluster in an image. . Edge detection is a well-developed field on its own within image processing. Relation between Region boundaries and edges are close, since there is often a sharp adjustment in intensity at the boundary region. Therefore Edge detection techniques been used as the base for another segmentation approach for sharp segmentation. The edges traced by edge detection are often discontinuous. For segmenting an object from an image with high complexity however, one needs closed connected region boundaries. The desired edges are the boundaries of such objects. Segmentation approaches can also be applied to already traced edges using edge detectors for more sharp edges. . In region-based methods, a lot of literature has investigated the use of primitive regions as a preprocessing step for image

segmentation. The advantages are twofold. First, regions carry on more information in describing the nature of objects. Second, the number of primitive regions is much fewer than that of the pixels in an image and thus largely speeds up the region-merging process. . Region based methods are based continuity. These techniques divide the entire image into sub regions depending on some rules like all the pixels in one region must have the same gray level. Region-based techniques rely on common patterns in intensity values within a cluster of neighboring pixels. The cluster is referred to as the region, and the goal of the segmentation algorithm is to group the regions according to their anatomical or function roles.

II. LITERATURE REVIEW

2.1 Automatic image segmentation by dynamic region merging

In this paper it addresses the problems with region merging. Where it start with an over segmented region in which many super pixels with homogenous color are detected hence image segmentation is performed iteratively merging the region according to the statistical way. There are two issues in region merging style one is stopping criteria and other is order of merging. Stopping criteria means exactly we can't conclude that where we need to stop the loop an order of merging is the state that where we need to merge region in order to form a large region. Problem in this paper is solved by sequential probability ratio test (SPRT) Algorithm that are used where dynamic region merging minimal spanning tree, region based algorithm and region adjacency graph. Advantage of the paper is that the neighboring regions with coherent colors are merged into one, boundaries are well located on the reasonable places and algorithm can tolerate variations for grouping meaningful regions in an image. Hence with the final results and discussion came limitations were found such as they may miss some long but weak boundaries, it may also merge region with short but high contrast boundary random nature of sequential probability ratio test might lead to non unique partitions to an image. Hence the future work of the paper was to deal with regions which are suppressed by other dominant region.

2.2 Improving fuzzy algorithm for automatic image segmentation.

In this paper it deals with the questions of fuzzy algorithm i.e. can the fuzzy k-means (FKM), kernel zed FCM (KFCM) and spatial constrained (SKFCM) work automatically without pre-define clusters. Hence they had present automatic fuzzy algorithms with considering some spatial constraints on objective function. Hence the existing work of the paper deals with fuzzy algorithms which are used for MRI segmentation and algorithms by considering some spatial constraints on the objective function. Segmentation is used for the brain web merging. Their proposed work deals with the same algorithm which is modified to produce the effective results hence their output was calculated and compared with the existing algorithms. The algorithms which are used are fuzzy k-means (FKM), fuzzy c-means (FCM), and kernalized FCM (KFCM) spatial constraints (SKFCM). The advantages of these algorithms where it estimates the correct tissues and more accurately, noise was reduced the modified algorithms where much faster, it viewed the high robustness in discrimination of the region because of low level of signal/noise ratio. But yet it has found certain limitations such as it consume much time for obtaining the true number of segments, accuracy was not improved and computational speed of segmentation was reduced. Hence the future work was to overcome with the limitations.

2.3 A fast interactive image segmentation to locate multiple similar-colored objects.

Many conventional image to some extent suffer from the problem of inaccurate segmentation. In this paper they had proposed the fast and simple technique for interactive image segmentation. The existing work was done on images with different color background. And the proposed work was carried out in three steps first it deals with the pre-segmentation by some low level segmentation method second was with the region marking where the region with similar features was marked under one region and third was region labeling the regions where labeled. The algorithm used in this paper where mean shift analysis watershed algorithm which is based on region merging than the interactive image segmentation method (MSRM). By proposed algorithm it deals with many problems such as it has capability to identify the multiple similar objects, the regions which are closed to the background were retained and the foreground regions are maintained efficiently. But yet it has some limitations such as unwanted regions were merged and secondly the proposed methods were based on threshold not on adaptive method. Hence to deal with this problem the proposed work was to extend the method to adaptive.

2.4 Dynamic ISAR imaging of maneuvering targets based on sequential SL0.

ISAR imaging is widely used in many military and civilian applications including target recognition, aircraft control and air/space surveillance. Hence in this paper they had represented the dynamic algorithm for ISAR imaging based on the sequential processing of smoothed L0 (SL0) which is one of the most effective SR algorithms in the complex domain. Hence the existing work deals with the SAR images i.e. locating the SAR images an working on them the proposed work deals with the L0 filter and working them on SAR images the algorithms which were used such as sparse recovery algorithm, L0 filter, Fast Fourier transform hence the advantages of this algorithms were that when SAR is used with the L0 there is no blurring and high resolution is obtained, and hence the processing time is decreased. But yet it has found some disadvantages such as L0 is more complex to implement. The processing time was increased when the ISAR images are used with the FFT. Hence from the results and discussion it was stated that the modeling cross range compression in the matrix form, the SSL0 algorithm in the complex-valued domain is proposed for the fast recovering the ISAR image sequentially. The similarity between two adjacent ISAR images are defined as the stopping rule and the minimum pulse number required in each CPI can be determined. Simulation results show that the proposed algorithm is promising from practical considerations.

2.5 Tree-pruning A new algorithm and its comparative analysis with the watershed transform for automatic image segmentation.

Tree pruning and watershed (WS) has been presented in the framework of the image forest transform (IFT). Hence in the proposed work tree pruning was introduced and then it was compared with the water shed. Algorithm which was used were watershed, tree pruning and image forest transform(IFT). Advantages of this paper was the tree pruning was more robust and provides image segmentation with higher accuracy secondly problem related to image segmentation such as boundaries are weak, image is noisy and blur were reduced. To obtain the accurate results future work can be improved by combining tree pruning with statistical approaches.

2.6 Improved techniques of automatic image segmentation

Several techniques have been developed for image segmentation the watershed algorithm which is important morphological tool for image segmentation has been widely used. This technique is a region growing algorithm

that analyzes an image as a topographic surface. Object oriented processing has recently been introduced to image and video processing hence object based coding provides more functionality to video like object manipulation and the combination of natural and synthetic video. Thus image or video segmentation is an important field of research in video processing. Hence in this paper it mainly deal with image but techniques are applicable to video signals. Hence the existing work is carried out in three steps simplification, marker extraction and boundary decision simplification which make use of area morphology and hence removes unnecessary information from the image to make it easy to segment. Marker extraction identifies the presence of homogenous region and a new marker extraction design is proposed in both forms that is luminance and color information and watershed algorithm was modified and boundary decision was based on region growing algorithm. Algorithms which was used where region growing algorithm watershed algorithm and morphological filter are used. The main advantage of this method was that their edges were maintained but great loss of information was noticed.

2.7 Automatic image segmentation by integrating color-edge extraction an seeded region growing.

In this paper they state the new automatic image segmentation method in which the color edges are first obtained automatically by combining an improved isotropic edge detector and a fast entropic thresholding technique. The initial seed for this region is captured by obtaining color edges which have provided the major geometric structures in an image and the centroids between these adjacent edge regions. These seeds are than replaced by the centroids of the generated homogenous regions. The algorithm which was used are the color edge extraction and facial extraction in which the color edge extraction detects the different color from the images and seprate them by labeling the different regions and facial extraction was done to state the facial characters the advantages of this technique was they could detect the homogenous region with accurate boundaries but limitations was that they may leave discontinuity in an image hence their future work was to deal with an image to form continuous image.

2.8 A robust automatic clustering scheme for image segmentation using wavelets.

The objective of this paper is to divide an image into homogenous region which is made up of complex textures. Hence the approach which has been suggested is spatial frequency techniques. Proposed methodology deals with automatically selecting the optimal features for each pixel using wavelet analysis. The algorithm used were robust segmentation algorithm and optimal region for segmentation . The advantage of this technique Were it requires no threshold and is completely automatic. Its limitation was to determine the optimal no of regions.

III. COMPARISON OF PAPERS AND THEIR TECHNIQUES

	Image is noisy	Background is retained	Boundaries are well defined	Pixel are peculiar	Blur image	Resolution of image	Well defined image	Loss of information
Paper (a)	NO	NO	NO	YES	NO	HIGH	YES	Chances are low
Paper (b)	NO	YES	YES	YES	NO	HIGH	YES	NO
Paper (c)	NO	YES	YES	YES	NO	MEDIUM	YES	CHANCES ARE LOW
Paper (d)	NO	YES	YES	YES	NO	HIGH	YES	NO
Paper (e)	YES	YES	NO	YES	YES	HIGH	YES	YES
Paper(f)	YES	YES	YES	NO	YES	LOW	NO	YES
Paper (g)	YES	YES	YES	NO	YES	HIGH	NO	YES
Paper (h)	NO	YES	YES	YES	NO	HIGH	YES	YES

Table 1 : COMPARISON OF TECHNIQUES**IV. LIST OF CHALLENGES**

Hence above papers are related to image segmentation and their region merging process comparing these papers we had come across various challenges that we need to work on. Such as

- Weak boundaries are not determined hence we may miss them.
- Region may get merge with short but high contrast boundaries.
- Images found are blur with no high resolution.
- Background is not retained and hence image is noisy.

V. CONCLUSION & FUTURE SCOPE

Here by comparing the papers we found that fast interactive image segmentation to locate multiple similar colored objects is better than other methods. But still it has some drawbacks such as loss of information and resolution of image is low. So in our future work we deal with this problem by using L0 smoothening filter.

REFERENCES

- [1] Bo Peng, Lei Zhang, and David Zhang, Fellow, Automatic image segmentation by dynamic region merging, IEEE transaction on image processing, VOL, 20, pp 3592-3604 December 2011.
- [2] Zhen Liu, student, peng You, Xizhang Wei, and Xiang Li, Dynamic ISAR Imaging of Maneuring Targets Based on Sequential SL0, IEEE geosciences and remote sensing letters VOL 10, pp 1041-1045, September 2013.
- [3] Hai Gao, Wan-Chi Siu, and Chao-Huan Hou, Improved techniques for automatic image segmentation, IEEE transactions on circuit and system for video technology, VOL 11, pp 1273-1280, December 2001.

- [4] Robert Porter and Nishan canagrajah, A robust automatic clustering scheme for image segmentation using wavelets IEEE transactions of image processing VOL 5, pp 662-665, APRIL 1996.
- [5] Jianping Fan, David K.Y. Yau, Ahmed. K. Elmagarmid senior, and Walid G. Aref, Member, Automatic Image segmentation by integrating color-Edge Extraction and seeded region growing. IEEE transaction on image process-ing VOL 10,pp 1454-1466 , October 2001.
- [6] Paulo A.V. Miranda, Felipe P.G. Bergo, Leonardo M. Rocha, Alexandare X. Falcao. Tree pruning: A new algorithm and its comparative analysis with the watershed transform for automatic image segmentation. Symposium on computer graphics and image processing.
- [7] E.A Zanaty, sultan aljahdali. Improving fuzzy algorithms for automatic image segmentation. College of computers and information technology.
- [8] Bibhas Chandra dhara bhaptosh chanda. A fast interactive image seg-mentation to locate multiple similar colored objects 2011 third national conference on computer vision, pattern recognition, image processing and graphics.

SYNTHESIS, CHARACTERIZATION AND TRANSPORT PROPERTIES OF PANI WITH CdO COMPOSITES

Manjula V T¹, Basavaraja Sannakki², MVN Ambikaprasad³ and
Chakradhar Sridhar⁴

^{1,2,3,4}Department of Post Graduate Studies and Research in Physics,
Gulbarga University, Kalaburagi, Karnataka(India)

ABSTRACT

The composites of polyaniline (PANI) with cadmium oxide (CdO) at different weight percentage were synthesized by insitu chemical oxidation polymerization method using Ammonium peroxydisulfate (APS). As an oxidizing agent and characterized using X-ray diffractometer to investigate amorphous or crystalline nature. From XRD it is found that polyaniline is amorphous in nature and composite is in crystalline in nature and CdO is uniformly distributed in the PANI. SEM images confirmed that size particles of PANI and its composite is in the range of 65-170nm. Further the dielectric constant, dielectric loss and AC conductivity are studied as a function of frequency at room temperature. The dielectric constant, dielectric loss decreased as frequency increased and after 10 KHz they almost remain constant.

AC conductivity increased after 10 KHz as frequency increased.

Key words: *A C conductivity, Dielectric constant, Dielectric loss, polyaniline composite, SEM and XRD*

I. INTRODUCTION

Nowadays conducting polymers are popular in the field of materials science due to their potential applications in many electronic devices [1-6]. Polyaniline is one of the important conducting polymers because of its solubility in some organic solvents leads to change in its electronic structure and physical properties by both charge transfer doping and protonation [7-11]. In general the change in properties makes polyaniline a versatile material. Polyaniline have the best combination of environmental stability, good conductivity and low cost. Particularly change in electrical properties of polyaniline with applications such as active electrode in batteries, in microelectronics, sensors, energy storage elements, organic light emitting diodes, as electro chronic material for displays, etc. In the present work the composites of polyaniline with CdO at different weight percentage were synthesized by chemical polymerization method using ammonium persulphate as an oxidizing agent. Cadmium oxide (CdO) is n-type semiconductor and has been used in application such as photo diodes, phototransistors, photovoltaic cells, transparent electrodes, liquid crystal displays, IR detectors etc. CdO microparticles undergo band gap excitation when exposed to UV light. With this background of multifunctionality CdO is used in composite preparation [12-13]. The formation of PANI/CdO composites were characterized by XRD and SEM. The properties such as dielectric permittivity, dielectric loss and A C conductivity of PANI/CdO composites have been studied as function of frequency in the range of 50 Hz to 50 MHz at room temperature.

II. EXPERIMENTAL MEASUREMENTS

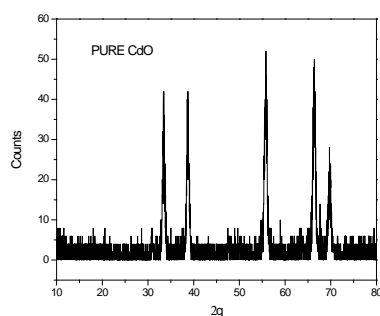
2.1 SYNTHESIS OF SAMPLE

The chemicals of aniline monomer, Ammonium per sulfate (APS)(NH₄)₂S₂O₈, hydrochloric acid (HCl), and CdO were procured from Sd fine Chemicals Mumbai. The chemicals used were of analytical reagent (AR) grade. Aniline of 0.0548 mol was dissolved in 1M HCl to form aniline hydrochloride. CdO was added in different wt% to the above solution with vigorous stirring to keep CdO suspended in the solution. To this above reaction mixture the oxidant solution which was prepared by dissolving 0.022mol APS in 50 ml of distilled water, added drop wise with continuous stirring for about 2 hrs and the resulting mixture is kept overnight to polymerize completely. After one day the resulting precipitate is filtered and washed repeatedly with deionized water and finally the resultant precipitate was dried in an oven for 8hrs at 60 degree temperature. The dried powder of polyaniline with CdO composite is used to make a pellet by applying 5-6 tons of pressure using a pellet making machine [Model-UTM]. The silver paste is coated on both sides of surface of the pellet for providing electrical contacts. The pellets are used for experimental measurements of capacitance, dissipation, impedance and phase angle using computer interfaced LCR Q-meter [Model: HIOKI 3532-50].

III. RESULTS AND DISCUSSION

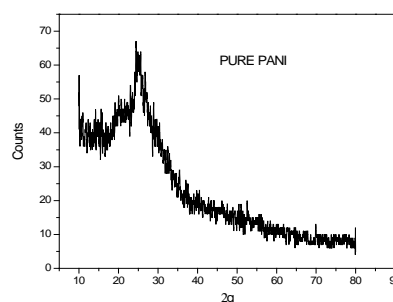
3.1 XRD and SEM Characterization

The CdO in the form of powder is used for XRD measurements using powder method of X-ray diffractometer [Model: Regaku]. The XRD spectrum is given in Fig 1. The peaks are occurred for CdO at an angle of $2\theta = 34, 39, 56, 67, 70$ degrees which shows the crystalline nature. The powder of polyaniline is used for XRD and the spectrum is given in Fig 2. It is noticed from Fig 2 that a broad and diffused peak observed at an angle $2\theta = 26$ degree. This shows polyaniline is amorphous in nature. The XRD spectrum for the composite of polyaniline with CdO is given in Fig 3. The peaks are occurred for the composite of polyaniline with CdO at an angle of $2\theta = 38, 44, 65, \text{ and } 77$ which shows the composite has crystalline in nature and there is modification in the structure of the composite.



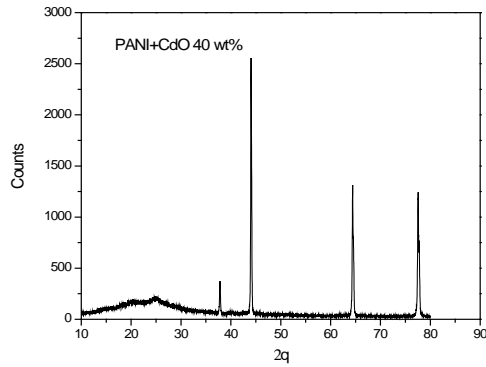
(1)

Fig.1: XRD spectra of pure CdO.

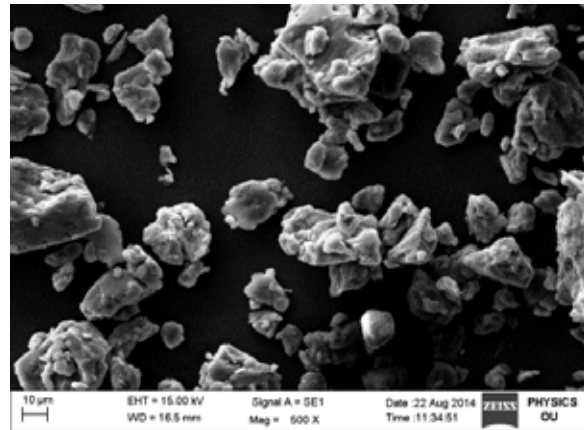


(2)

Fig.2: XRD spectra of pure PANI



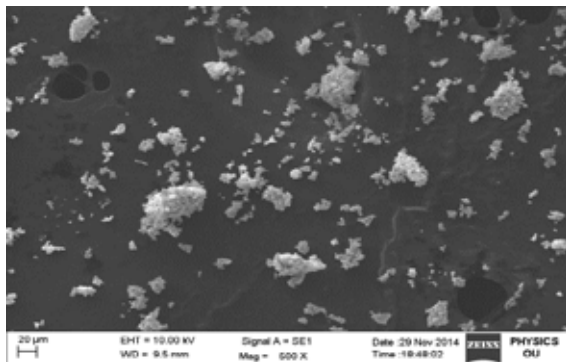
(3)



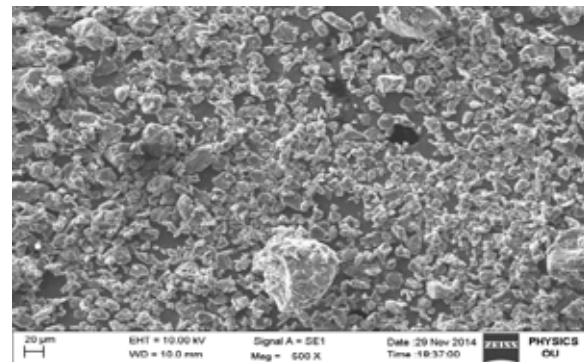
(4)

Fig.3: XRD spectra of PANI/CdO composite.

Fig 4: SEM Images of PANI.



(5)



(6)

Fig. 5: SEM image of CdO.

Fig. 6: SEM IMAGE OF composite of PANI/CdO at 40 wt %

The SEM image of PANI, CdO and PANI/CdO composite is shown in the Fig (4-6). It can be confirmed that particle size is in nanometer. The size of particles in polyaniline is around 65nm and PANI/CdO composite is around 170nm. The SEM image also reveals that homogenous distribution of CdO in polyaniline.

3.2. Transport Properties

3.2.1 Dielectric Constant

The dielectric constant as function of frequency for PANI/CdO composites at room temperature is studied using the equation

$$\epsilon_r = \frac{Cd}{\epsilon_0 A} \quad (1)$$

Where C is capacitance, d is thickness of the sample, A is area of the sample and ϵ_0 is the permittivity of free space. Fig. 7 shows the variation of dielectric constant with frequency at different wt%. The dielectric constant decreased exponentially as frequency increased. After 10 KHz it shows frequency independent behavior it is because of electrical relaxation process. From the graph we can see that after the addition of CdO the dielectric constant at lower frequency further increases and exponentially decreases up to 10 KHz after that shows frequency independent nature except 10wt%.

3.2.2. Dielectric Loss

The dielectric loss as function of frequency for PANI/CdO composites at different weight percentages are obtained with help of the measured data of dissipation and the values of dielectric constant using the equation given by

$$\epsilon'' = \epsilon' \tan \delta \tag{2}$$

Fig 8 shows the variation of dielectric loss as a function of frequency at room temperature. Here also we can see that dielectric loss for PANI and its composite with CdO goes on decreases exponentially up to 10 KHz after that it shows frequency independent behavior.

3.2.3 AC Conductivity

The AC conductivity (S_{ac}) as function of frequency for the polymer of PANI and for its composites with CdO at different weight percentages are obtained with help of values of the dielectric constant and dielectric loss using the equation given by

$$S_{ac} = \epsilon_0 \epsilon' \omega \tan \delta \tag{3}$$

Fig 9 shows variation of AC conductivity as a function of frequency at room temperature. From Fig it is found that AC conductivity remains constant up to 10 KHz after that it goes on increasing exponentially. Further the addition of Cdo increases AC conductivity except 10 wt %. It is because of at higher frequency all the dipoles are aligning in one direction also the extension of chain length of PANI where the polarons get sufficient energy to hop between favorable localized sites.

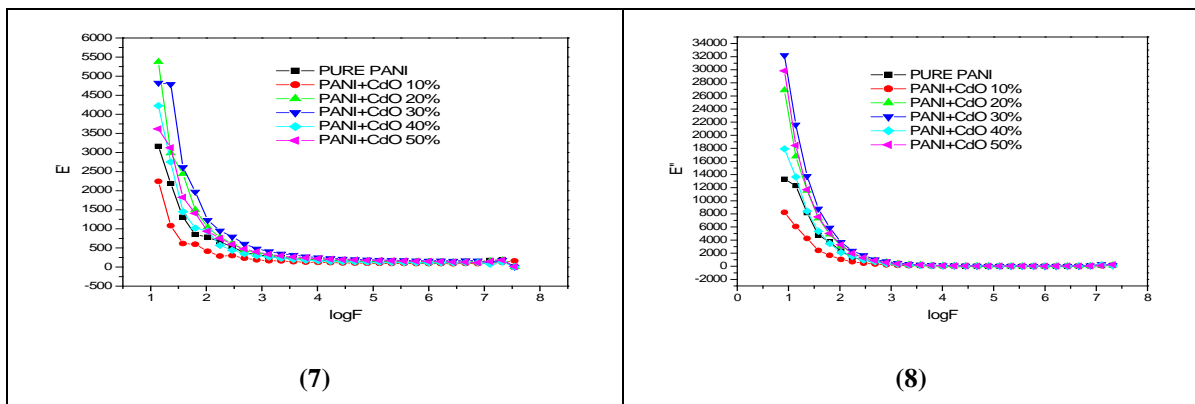


Fig.7: Plot of logf vs dielectric constant.

Fig.8: Plot of logf vs dielectric loss.

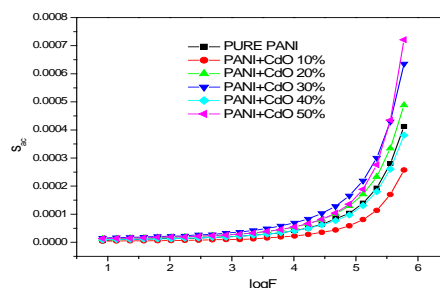


Fig.9. Plot of logf vs conductivity

IV. CONCLUSION

The conducting polyaniline and its composite with CdO have been synthesized successfully using chemical oxidation method. The XRD spectrum for the composite of polyaniline with CdO is crystalline in nature. The peak positions are also differs from the pure CdO and this indicates the modification in the structure of the composite. The values of dielectric constant and dielectric loss have been increased at lower frequency region after addition of CdO. A remarkable increase is seen in AC conductivity with the addition of Cdo. From the SEM it can be confirmed that particle size is in nanometer, also reveals that homogenous distribution of CdO in polyaniline.

REFERENCES

- [1] A.G Mac Diarmid, J. C Chiang, M. Halpun, W.S Huang,S.L . Mu, N.L.D. Somarisi, W.Wu and S.I Yaniger: Mol.Cryst Liq. Cryst.vol-121 pp-173(1985).
- [2] A.G Mac Diarmid, J. C Chiang, A.F Ritcher and A. Epstein: Synth. Met. Vol-18,pp-285(1987).
- [3] H.Naarman: Adv. Mater.vol-2 pp-345(1990).
- [4] G. Kumar, A.Sivashanmugam,N Muniyandi ,S.K. Dhavan & D.C. Trivedi: Synth Met, vol-80, pp-279 (1996).
- [5] M.K. Song ,I.J. Won & H.W. Rhee: Mol Cryst Liq Cryst , vol-337 pp-316(1998).
- [6] M.Kurian ,M.E.Galvin,P.E. Trapa,D.R. Sadoway & A.M. Mayes: Electrochemica Acta, vol-50 pp-2125 (2005).
- [7] M. Angolopoulos ,G.E. Asturias ,E. Ermer ,S.P. Ray,E. Scher and A.G Mac Dermid: Mol .Cryst .vol- 160 pp-151 (1998).
- [8] W.H.Kim,A.J.Makinen,N Nikolov, R.Shashidhar,H.Kim & Z.H.Kafafi: Appl Phys Lett, vol-80 pp-3844 (2002).
- [9] S.Tokito,M. Suzuki & F.Sato: Thin Solid Films,vol-353 pp-445(2003).
- [10] S.C.Jain, T. Aernout, A.K.Kapoor, V Kumar, W. Geens, J. Poortmans, & R.Mertens: Synth Met,vol 245 (2005).
- [11]H.Etori, X.L.Jin,T.Yosuda, S.Mataka, & T. Tsutsui: Synth Met,vol-156 pp-1090 (2006).
- [12]Ashis S Roy,Koppalkar R,M V N Ambika Prasad:Journal of applied polymer science,Vol.123,pp-1928 (2012).
- [13]Subhash Kondavar,Ritu Mahore,Ajay Dahegaonkar,Shikha Agrawal:Adv.Appl.Sci.Res.vol-2(4) pp-404 (2011).

DETERMINATION OF ENERGY LOSS, RANGE AND STOPPING POWER OF LIGHT IONS USING SILICON SURFACE BARRIER DETECTOR

Mahalesh Devendrappa¹, R D Mathad² and Basavaraja Sannakki³

^{1,3}Department of Post Graduate Studies, ²Research in Physics,
Gulbarga University, Kalaburagi, Karnataka (India)

ABSTRACT

Energy loss of light ions, such as alpha particles of energy 5.15 MeV [Pu-239], has measured in atmospheric air at different pressures. Experimentally, the energy loss measurement was made using Silicon Surface Barrier Detector (SSBD) of an alpha ray spectrometer. Silicon Surface Barrier Detector has a higher resolution of 20 KeV at energy of 5.15 MeV. The alpha source and the detector were kept at a fixed distance of 10 mm. The measured energy loss in the air medium has higher than that in vacuum. The value of energy loss in atmospheric air at a pressure of 4.6 mbar is 0.8639 MeV, and calibrated energy loss in vacuum is 8.93 KeV per channel. The stopping power of alpha particles decreased exponentially as transmitted energy increased in the energy range of 2.0-6.0 MeV. The nuclear and electronic energy loss stopping powers are studied as a function of transmitted energy of alpha particles in atmospheric air using SRIM values.

Keywords: Alpha Particles, Energy Loss, Range, SSB Detector SRIM and Transmitted Energy

I. INTRODUCTION

The energy loss of ions passing through matter has been the subject of exhaustive studies starting from the classical effort of Bohr, Bethe and Bloch and still ruins motivating now. The study of the passage of fast-moving particles through matter has been important, since from the early days of nuclear physics. For light ions, such as $^4\text{He}^+$ penetrating through a solid, the energetic particles lose their energy (Northcliffe and Schilling 1970, Hubert et al 1990 Ziegler 1999) primarily thorough the excitation and ionization in the inelastic collision with atomic electron termed as electronic energy loss. Microscopically, energy loss due to excitation and ionization is a discrete process. However, macroscopically, it is a good assumption that the moving ions lose their energy, continuously. We considered the average energy loss during the penetration of ions into a given material. The measured energy loss must be determined with the distance Δt or the thickness of the thin films, the ions will would travels through the target or thin films. The ions lose their energy, while passing through the target, which depends on the Mass Density (ρ) or Atomic density (N). The Mass Density and Atomic density together give rise to the Energy Loss of the target material i.e. $\rho\Delta t$ or $N\Delta t$. Silicon Surface Barrier Detectors (SSBDs) have already been used in the fields of charged particle detection as a target for coherent interaction in a series of experiments by Bellini et al [1]. Yuan was probably first to use them for detection of charged particles. But, in general the solid state detectors have been used scanty for high energy physics experiments. Because, they cannot provide large detecting area, which is required in common Spectrometers. A need is required now for the thin particle detector very near to the interaction region with high precision high rate and

high multiplicity capacity, which is difficult to meet with existing detectors. Especially, the study of very short lived charged particles will profit for an electronic detector in the target region [2]. The SSBDs are fabricated with N-type silicon with resistivity in the range 1000-8000 ohm-cm, the silicon wafer after lapping to remove the surface damage created by crystal slicing process is cleaned with organic solvent[3]. The electrical contacts are made with gold evaporation on the P-type surface and with aluminum on the N-type back surface provides on ohmic contact detectors is encapsulated with BNC or microdot connector. Si is one of the extraordinary semiconductors suited for the fabrication of high-quality radiation detectors by virtue of high-quality Si wafer production and stable semiconductor process technology. With a band gap of 1.1eV at room temperature, the intrinsic concentration of charge carriers is low, thus avoiding excessive noise. Charge carrier lifetimes and mobilities are high, which is necessary for low noise detectors with a good timing behavior. Silicon surface barrier (SSB) radiation detectors are widely used in experimental nuclear physics for the spectroscopy of alpha particles, heavy ions, and fission fragments.

1.1 Silicon Surface Barrier Detector

There are three main parameters that define a silicon surface-barrier detector: resolution, active area, and depletion depth. The ORTEC model numbers reflects these three parameters in its model in the same order. The R-018-450-100 detector which defines its parameters on its model as; The R stands for Ruggedized detector with a resolution of 18 KeV for 241Am alpha particle, an area of 450 mm², and a depletion depth of 100 μ m. It operates with 0-200 bias voltage, which can be varied by ALSS software [4]. Figure.1 shows the schematic diagram of experimental set up and circular disc detectors, its active area defines the diameter of its faces at any given distance from the source; a larger area will subtend a larger angle and thus intercept a greater portion to the total number of alpha particles that emanate from the source. The depletion depth is synonymous with the sensitive depth of the detector. For any experiment the depth must be sufficient to completely stop all the charged particles that are to be measured, and its ability to do this is dependent upon both the energy and the particle type. Note that a 5.5 MeV alpha is completely stopped with about 27 μ m of silicon [5]. Since, natural alphas are usually less than 8 MeV in energy; a 50- μ m detector is adequate to stop all natural alphas.

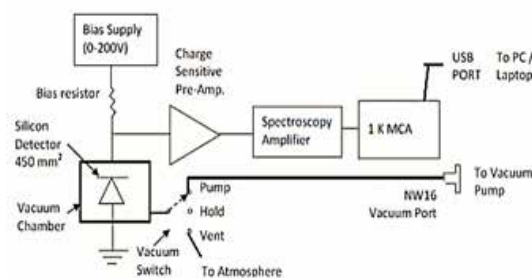


Fig.1: Schematic diagram of experimental set up.

Inadequate, thickness uniformity of totally depleted ΔE detectors has undoubtedly been responsible for many disappointing experiments. A 10-MeV ⁴He particle incident on a 50- μ m-thick silicon detector will lose approximately 5.9 MeV in traversing the detector. The rate of energy loss (dE/dx) of the exiting particle, however, will be about 160 KeV/ μ m. This means that a detector thickness variation of 1 μ m would cause an energy spread of 160 KeV.

1.2 Bohr's Theory

This theory was anticipated by Bohr in 1948 it is based on the assumption that the incident ions are fully stripped and their energy loss in the target material is very small as compared to the incident ion energy [6]. According to this theory, the calculations of straggling standard deviations, Bohr developed the following expression.

$$(W_B^2) = 4P (Z_1)^2 e^4 Z_2 N x \quad (1)$$

Where Z_1 and Z_2 are the atomic number of incident ion and target material respectively, e is the electronic charge, N is the number of target atoms per unit volume and x is the target thickness.

II. EXPERIMENTAL MEASUREMENTS

The experiment has carried out using passivated ion-implanted planar SSBD of resolution 20 KeV in vacuum for alpha particles [Pu-239] of energy 5.15 MeV connected with vacuum chamber using hosepipe. The operating voltage of +30 volts was applied to the SSBD detector through software of an alpha ray spectroscopy. The rise and fall times were < 100 ns and 100 μ s, respectively and output of +100 mV for 5.15 MeV for low noise charge sensitive preamplifier. The detector connected with vacuum chamber was made with solid brass Nickel plating for ease of decontamination and high performance O-ring seal. The internal dimensions of the scattering chamber were 61 mm wide x 74 mm deep x 40 mm height where the detector is to be kept. The sample spacing is from 2 mm to 40 mm in steps of 4 mm, The vacuum inside the scattering chamber can be controlled using the hold and vent valves[7,8].

The alpha particles with initial energy E_1 enters into the medium [9] While, E_2 being the transmitted energy after the medium. The energy loss [ΔE] of alpha particles can be obtained using equation. 2.

$$\Delta E = E_1 - E_2 \quad (2)$$

The stopping power per unit length relation is given by following equation.3.

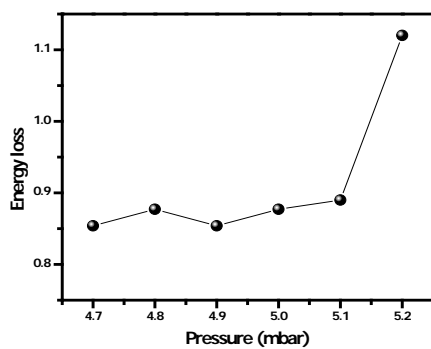
$$\Delta E / \Delta X \text{ Or } dE/dx \quad (3)$$

The experiment was performed using passivated ion-implanted planar SSBD of resolution 20 KeV in vacuum, 5.5 MeV energy, system resolution better than 30 KeV for Pu-239 and efficiency is >25% for detector source spacing of < 10mm for Pu-239 at operating voltage +30 Volts.

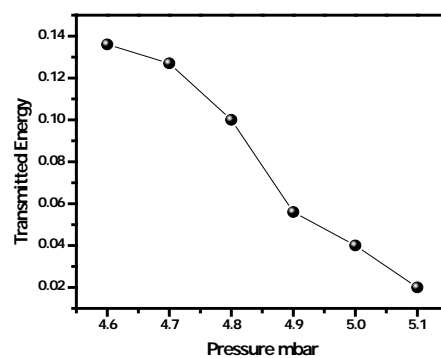
III. RESULT AND DISCUSSION

The measured energy loss in atmospheric air at a pressure of 4.6 mbar is 0.8639 MeV. The energy calibration has done using Alpha source of energy 5.15 MeV which gives energy of 8.93 KeV per channel. The computed stopping power is 0.01799 MeV/mm using SRIM. In the vacuum medium, the number of particles in the scattering chamber was decreased by creating more vacuum in the scattering chamber using the rotary pump. The energy loss of alpha particles at different pressures of the vacuum medium is shown in figures. As the pressure in the vacuum chamber increases, the alpha particle energy peaks widen. This is due to energy straggling, a process where statistical fluctuations occur in the number of collisions along the path of the particles and in the amount of energy lost per collision. It is observed from figure 2.that as the pressure in scattering chamber increases the energy loss of the alpha particle increases gradually. This was ascribed to the lesser interaction of alpha particles with the medium. At higher pressure, the scattering chamber possesses more

number of gaseous molecules in the traversing path of the alpha particle ions and hence the probability of the interaction will be more. As a result, this leads to a more energy loss of alpha particles in the medium. Consequently, the transmitted energy of alpha particles is high at higher pressure but whereas at lower pressure the transmitted energy is less. This is due to the more number of molecules present in the scattering chamber and that result in the probability of interaction of the alpha particles with these molecules is higher and that gives the lesser transmitted energy which is given in figure 3. The figure 4 and 5 shows a plot of nuclear and electronic energy loss, in atmospheric air, as a function of projected energy of alpha particles in the energy range of 2-6 MeV, were using SRIM [Verson-2008]. This graph reveals that as projected energy of the alpha particles increases the nuclear energy loss decreases exponentially. This is due to the interaction mechanism by which the ion can lose energy by elastic collision with the nuclei of target atoms of atmospheric air media.

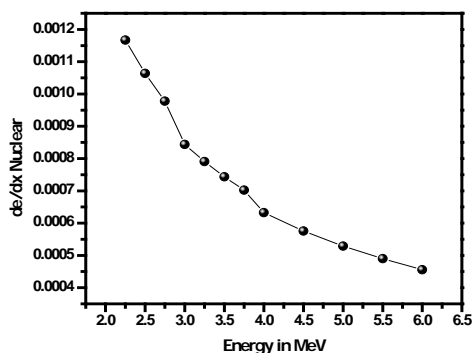


(2)

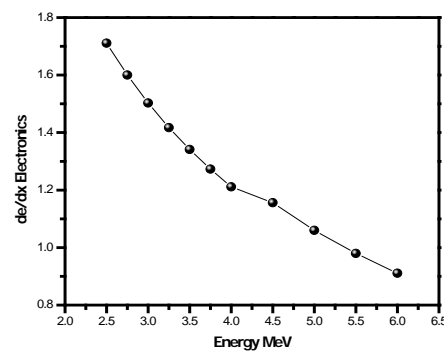


(3)

Fig.2: Plot of Pressure Versus Energy Loss of Alpha Particles In Atmospheric Gas. Fig.3: Plot of Pressure Versus Transmitted Energy Loss of Alpha Particles In Atmospheric Gas.



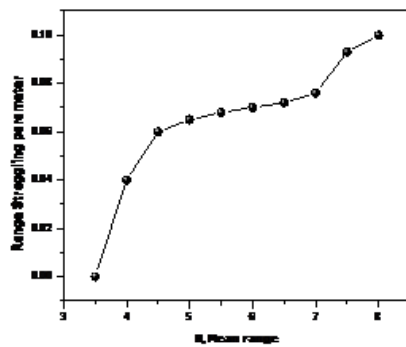
(4)



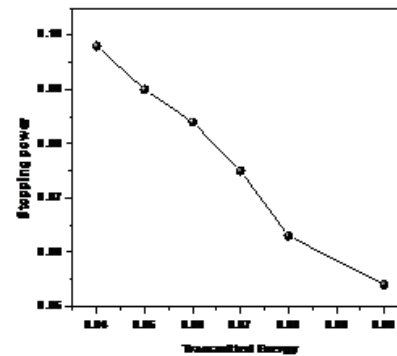
(5)

Fig.4: Plot of Projected Energy Versus Nuclear Energy Loss In Gas Using SRIM Code. Fig.5: Plot of Energy Versus Electronic Energy Loss In Gas Using SRIM Code.

The figure 6 shows energy verses projected range and of alpha particles in atmospheric gas at room temperature from 3-8MeV. It shows that as mean range of ions increases due to statistical fluctuations in the scattering chamber this leads increase in range of alpha particles in the air. This is in concurrence with the results of both Comfort *et al*[23] and Mason *et al*[22] It is interesting to note that helium is the only gas for which the experimental results are much bigger than any one of the theoretical curves. The charge exchange phenomenon again offers a possible explanation of ions with different charges will lose energy at different rates.



(6)



(7)

Fig.6: Plot of Mean Range Versus Range Straggling Parameter of Alpha Particles In Atmospheric Gas. Fig.7: Plot of Transmitted Energy Versus Stopping Power of Alpha Particles In Atmospheric Gas.

Due to the capture and loss process an alpha particle will waste sometime in the singly charged state and sometime in the doubly charged state while passage the absorber. The time spent in one state or another will be different for different ions, and thus they will arrive at the detector with different energies; therefore, the net effect of the capture and loss process is to further broaden the distribution. It is reasonable to believe that charge exchange between alpha particles and the helium atoms will be relatively large since they have identical atomic excitation and ionization energies, eventually this leads to an anomalous large amount of straggling. The Figure 7 shows the transmitted energy verses stopping power (S_e) of an alpha particle at various pressures. It resulted that as transmitted energy of alpha particle increases the stopping power of alpha particles decreases exponentially due to increase in the molecules of alpha particles in the traversing path, inside the scattering chamber this leads comparison of electronic energy loss of gas molecules.

IV. CONCLUSION

In conclusion, the measured energy loss of alpha particles increases with an increase in the pressure inside the scattering chamber. It was due to the reduction of air molecules in the scattering chamber or in traversing path of the ions in the medium at higher pressures. This was resulted in a higher energy loss at high pressures. Further, the transmitted energy of alpha particles decreases exponentially as pressure decreases and that was resulted in the lower projected range of alpha particles. The Electronic, nuclear energy loss and range of alpha particles at atmospheric gas is also studied. In the case as transmitted energy of alpha particles increases the stopping power decreases exponentially. These results hold's good agreements with SRIM code computation.

V. ACKNOWLEDGMENT

The above said authors are greatly indebted to Dr J Sannappa, Department of Physics, Kuvempu University Shimoga, Department of Physics Gulbarga University, Gulbarga and UGC New Delhi for providing a financial assistance to the MRP project.

REFERENCES

- [1] G Bellini et al., Nucl. Instr. and Meth. (1973)pp-107.
- [2] J.F. Ziegler, J.M. Manoyan, Nucl. Instr. and Meth. B35 pp-215. (1988).

- [3] G. F. Knoll, Radiation Detection and Measurement (John Wiley and Sons, New York, pp- 354,.(1999).
- [4] Alpha Spectroscopy Catalog. pp.2-4,.(2011).
- [5] P.K. Diwan et al, Radiation Physics and Chemistry, vol-81pp. 1543–1546,. (2012).
- [6] N. Bohr, The penetration of atomic particles through matter. Kgl. Dan. Vid. Selsk. Mat. Fys. Medd. 18 (8), pp1–144.(1948).
- [7] W.H.Bragg, , and Kleeman, R.Philos. mag. vol-10 S318. (1905).
- [8] Alpha spectroscopy user manual pp.1-3.9(2011).
- [9] E.H.M. Heyne et al., Nucl. Instr. and Meth.vol-178 pp.331-343,(1980).
- [10]J.Lindhard, M.Scharff, Energy loss in matter by fast particles of low charge. Kgl. Dan. Vid. Selsk. Mat. Fys. Medd. Vol-27 (15), pp.1–32.(1953).
- [11]N.Bohr,Mat. Fys. Medd. Dan. Vid. Selsk. 18 ,pp-8 (1948).
- [12] B. Sannakki and D Mahalesh Int. Journal of Research in Enng and tech.vol-3, PP.286-289. (2014).
- [13]J. F. Ziegler Journal of Applied Physics/ Rev. App .Phys.Vol-85.pp1249-1272 (1999).
- [14]M.Zardo *et a*, Nucl. Instr. and Meth in Phys Resrch B. Vol-259, pp-836-840. (2007).
- [15]M. S. Livingston and H . A. Bethe, Rev . Mod. Phys . Vol-9, pp-245 (1937).
- [16]D. Jay Bourke and T. Christopher Chantele, Journal of Physical Chemistry A, vol-116, pp-3202-3205, (2012).
- [17]Mahalesh Devendrappa and Basavaraja Sannakki, Journal of the Instrument Society of India, Vol-44, pp- 248-251, (2014).
- [18]P. J. Quseph and Andrew Mostych, American jornal of Physics, vol-46, pp-742-744, (1978).
- [19]H. H. Heckman and P. J. Lindstrom, Phys. Rev. Lett . 22, pp-871, (1969) .
- [20]H. H . Andersen, H . Simonsen and H. Sorensen, Nucl. Phys. A vol-125,pp- 171, (1969) .
- [21]J. E. Turner, “Atoms, Radiation and Radiation Protection”,Wiley-VCH, 2007. ISBN: 3-527-40606-9.
- [22]D. L. Mason, R. M. Prior, and A. R. Quinton, Nucl. Instr. Methods vol-45, pp-41, (1966)
- [23]J. R. Comfort, J. F. Decker, E. T. Lynk, M. O. Scully, and A. R. Quinton, Phys. Rev. 150, 249 (1966).

REGENERATIVE SHOCK ABSORBER

Sethu Prakash S¹, Nidhin Abraham Mammen², Steve John³,

Varughese Punnoose Kochuparackal⁴, Tobin Thomas⁵

^{1,2,3,4}Student, Department of Mechanical Engineering, Saintgits College of Engineering, (India)

⁵Assistant Professor, Department of Mechanical Engineering, Saintgits College of Engineering, (India)

ABSTRACT

In the past decade, regenerative braking systems have become increasingly popular, recovering energy that would otherwise be lost through braking. However, another energy recovery mechanism that is still in the research stages is regenerative suspension systems. This technology has the ability to continuously recover a vehicle's vibration energy dissipation that occurs due to road irregularities, vehicle acceleration, and braking, and use the energy to reduce fuel consumption. A regenerative shock absorber is a type of shock absorber that converts intermittent linear motion and vibration into useful energy, such as electricity.

Conventional shock absorbers simply dissipate this energy as heat. Regenerative shock absorbers utilize piston cylinder arrangement or generation of electricity. Piston undergoes compression and expansion with movement of vehicle. The system is designed in SOLIDWORKS. When used in an electric vehicle or hybrid electric vehicle the electricity generated by the shock absorber can be diverted to its power train to increase battery life. In non-electric vehicles the electricity can be used to power accessories such as air conditioning. Several different systems have been developed recently, though they are still in stages of development and not installed on production vehicles. This could be used on electric or hybrid vehicles (or normal vehicles) to capture energy which would otherwise be absorbed and wasted, and then convert it into electricity. The regenerative shock absorbers can harvest the power in a continuous way. We analytically determine the pressure and velocity at 0.5Hz and 1Hz. A graph is plotted between pressure and velocity. Analysis is performed in CFD and values are determined.

Keywords - Shock Absorber, Vibration, Hybrid Vehicle, CFD, Damper

I. INTRODUCTION

It is known that automobiles are inefficient, wasting over 80% of the energy stored in the fuel as heat. Thus eight of every ten gallons in the vehicle's tank don't help propel the vehicle; they are burned to overcome losses in the system.

Automobile manufacturers have made costly strides to improve fuel economy. For example, regenerative braking is standard on many hybrid automobiles. Car manufacturers also spend a great deal of effort to reduce wing drag so as to improve fuel economy through streamlined, low drag automobile body designs. Manufacturers also use lighter, yet more expensive, materials to reduce vehicle weight to reduce fuel consumption.

This investigation looks into the most efficacious rotary hydraulic mechanism of harvesting energy from a vehicle suspension system. More specifically, it investigates the viscous nature of the working fluid in a rotary design regenerative shock for more effective power transduction. Custom apparatuses were fabricated for the

purpose of this investigation. Both dynamometer and vehicle retrofit testing were performed to evaluate the results of electrical generation.

Ebrahimi has proposed energy electromagnetic dampers that are capable of harvesting energy [1]. He employed existing suspension system and damper design knowledge to develop concept of electromagnetic dampers. The ultimate objective of this thesis is to employ existing suspension system and damper design knowledge together with new ideas from electromagnetic theories to develop new electromagnetic dampers. At the same time, the development of eddy current dampers, as a potential source for passive damping element in the final hybrid design, is considered and thoroughly studied. For the very first time, the eddy current damping effect is introduced for the automotive suspension applications.

Li et al. proposed the vibration to be damped by both oil viscosity and operation of an electrical mechanism [2]. A three stage identification approach is introduced to facilitate the model parameter identification using cycle loading experiment. This paper has reported a novel energy-harvesting hydraulic damper for simultaneously damping vibrations and harvesting energy. The vibration acting on the two terminals of a hydraulic damper was converted into amplified rotation of a hydraulic motor. The output of the motor was then connected to the rotor of an electromagnetic generator, thereby yielding considerable power. In the process, some of the energy of the vibration was dissipated by the oil flow and some by the electromagnetic generation. An analytical model was proposed to depict both the mechanical and electrical responses.

Wang et al. studied the mathematical modeling of the shock absorber system [3]. A dynamic model of a shock absorber was evaluated. The results indicate that hydraulic circuit configuration regularizes the hydraulic flow to improve the efficiency of hydraulic motor in low-speed or high-pressure. For effective energy regeneration and vibration dampening, energy regenerative suspension systems have received more studies recently. This paper presents the dynamic modeling and a test system of a regenerative shock absorber system which converts vibration motion into rotary motion through the adjustment of hydraulic flow.

We the group of young engineers found that, there is an impending need to make Non Conventional energy attain popular acclaim. This is also very essential to preserve the conventional sources of energy and explore viable alternatives like sustainable energy (the energy which we are already utilizing but for some safety of other uses we are suddenly wasting it, that can be reutilized), solar, wind and biomass that can enhance sustainable growth. What is more, such alternatives are environment friendly and easily replenishable. Therefore, they need to be thoroughly exploited with a functionally expedient, energy matrix mix. Adaptation of technology and employing them should be pursued right from this moment to have a head start, be informed of the barriers in technology applications of the renewable variety and synergizing them with the existing, traditional power production technology and T&D networks. It is known that in coming times, wind energy will be the most cost-effective renewable resource. Yet, it is doubtful if any individual technology would hold centre-stage. Thus we selected kinetic generator means the “Energy in motion when it is suddenly applied with a sort of obstacle, then according to Newton’s law for every action there is an equal and opposite reaction. Utilization of this reaction is the basic reason behind the selection of this project work.”

II. METHODOLOGY

2.1 Working of Regenerative Shock Absorber

This is a hydraulic rotary shock absorber, a device that converts vertical motion into rotary motion via a hydraulic motor. It includes a piston disposed for reciprocating motion within a cylinder as a vehicle’s suspension system deflects. Hydraulic fluid is contained within the cylinder. A first circuit is in fluid

communication with a first chamber in the cylinder on a first side of the piston, in fluid communication with a hydraulic motor and in fluid communication with a capacitive reservoir. Upon compression of the piston, hydraulic fluid passes through the hydraulic motor thereby turning a shaft thereby. A second fluid circuit is in fluid communication with a second chamber in the cylinder on the second side of the piston and also in fluid communication with the first chamber. Upon extension of the piston, hydraulic fluid passes from the second chamber to the first chamber. An electric generator is connected to the hydraulic motor shaft for generating electricity upon rotation of the shaft.

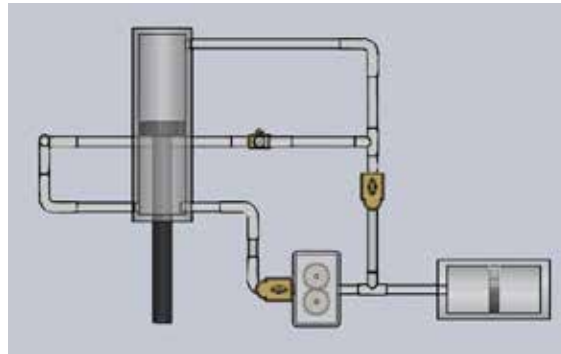


Fig. 1: Schematic Representation of Regenerative Shock Absorber

The device also includes a hydraulic circuit arrangement so that energy may be harvested during both compression and relaxation of the shock absorber. In this embodiment, upon compression or relaxation of the shock absorber, the resulting pressure differential across the hydraulic motor will induce rotational motion of its output shaft. This output shaft is directly connected to a permanent magnet generator or a DC electric motor. The wattage rating of the motor is selected entirely based on the vehicle's mass and spring stiffness.

The electrical energy generated may be used by the vehicle as it is generated or stored in, for example, the vehicle's battery. It is preferred that the harvested electricity be used to power components on a vehicle that would otherwise strain the internal combustion engine, thereby increasing fuel efficiency.

Beyond the basic fluid losses in the hydraulic circuits, damping is provided mostly by the electric generator as the counter-emf resists rotational motion of the armature relative to the stator. This resistance is transferred directly to the shock fluid by the hydraulic motor. The damping force provided by the motor is selected to be directly proportional to the velocity of the hydraulic fluid so that increased fluid velocity results in an increased damping force. The capacitive reservoir accommodates the piston shaft volume that is introduced upon the compression stroke of the shock absorber.

The model chosen to use is a simple spring-based model in which the energy that is present in the vertical motion of a car can be observed in the compression and extension of its springs. The energy in a compressed spring is given by the equation

$$E = \int F dx = \frac{1}{2} kx^2$$

Using an experimentally determined value for k of 1.2×10^5 N/m, we find that for a 3500 pound automobile, vertical displacements store the amounts of energy in a single spring as shown below. We note that heavy truck springs are much stiffer.

Table I: Potential Energy that can be harvested

1 cm displacement: 6 J	Summing over four wheels	24 J
3 cm displacement: 54 J		216 J
6 cm displacement: 216 J		864 J
9 cm displacement: 486 J		1994 J

We have approximated a normal city drive. Thus by assuming that the springs undergo vibrations of magnitudes 2 cm at a frequency 0.5 Hz and 1 Hz, keeping in mind that work is done both compressing and extending the spring so that energy can be harvested from both of these motions. Based on these assumptions, a one hour drive generates 1.34 kilowatt-hour of energy available to harvest.

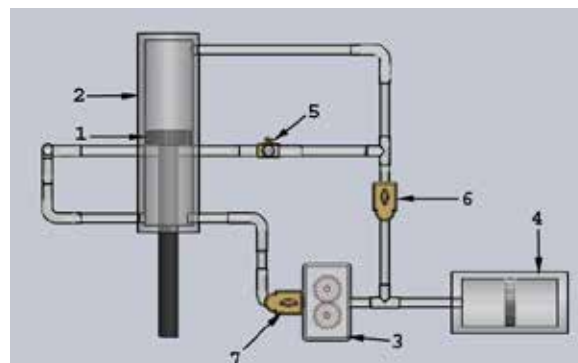


Fig. 2: Equilibrium Position of Regenerative Shock Absorber

With reference now to the drawing, Figure 2 illustrates the overall system in a first embodiment. Shock body 2 is a cylinder in which a piston 1 resides for reciprocating motion. Check valves 5, 6 and 7 control the flow of hydraulic fluid. The system also includes a hydraulic motor 3 and a capacitive reservoir 4.

As the piston 1 is compressed, pressurized hydraulic fluid builds in the top part of a chamber 8 and is passed through the check valve 6. Check valve 5 prevents the hydraulic fluid from flowing into a bottom chamber 9. After passing through the check valve 6, the fluid is directed into a hydraulic motor 3 and into a capacitive reservoir 4. The capacitive reservoir 4 acts to store any impulsive pressure surges and smoothes out the pressure of the hydraulic fluid as it is fed into the hydraulic motor 3.

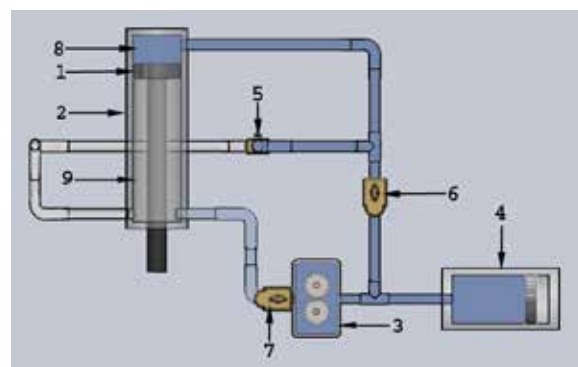


Fig. 3: Compressed Position of Regenerative Shock Absorber

With reference now to Figure 3, as hydraulic fluid passes through the hydraulic motor 3, it rotates the motor's shaft. The shaft of the motor 3 is coupled to a generator such as a permanent magnet generator. The output of the generator may charge a battery or power an automobile's electric systems when the hydraulic motor turns.

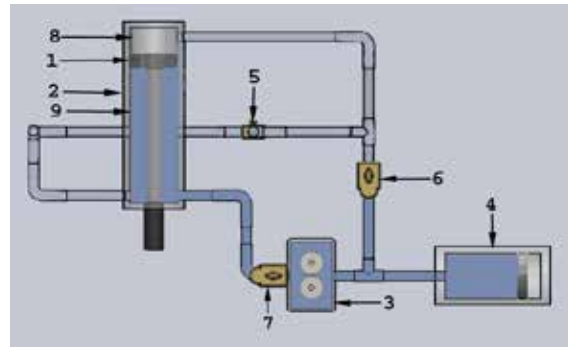


Fig. 4: Top Chamber Position of Regenerative Shock Absorber

Figure 4 illustrates fluid flow as the piston 1 extends. When the piston 1 moves downwardly, pressurized hydraulic fluid is compressed in the bottom portion of the chamber 9 and passes through check valve 5. Check valve 7 prevents the fluid from flowing back into the hydraulic motor 3. The fluid passing through the check valve 5 flows into the top chamber 8.

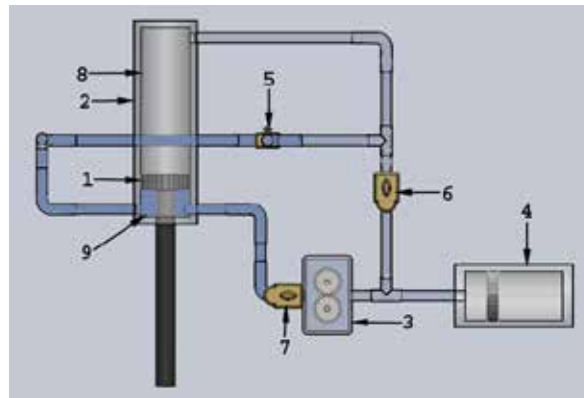


Fig. 5: Relaxation Position

Flow characteristics of at least one of the fluid flow circuits may be selected to provide an effective damping in addition to recovery of energy. In this way, the system of the invention not only provides for energy recovery, but also effective damping for wheel control, thereby eliminating the need for a conventional shock absorber. The regenerative shock absorber of the present invention is applicable to any wheeled vehicle; heavy trucks remain a compelling target because of their substantial weight and high suspension spring stiffness.

2.2 Working Fluid

The conversion of linear to rotary motion is the basic mechanism that enables this to harvest the wasted energy of a vehicle's suspension system. It is accomplished via hydraulics and the working fluid remains an essential component to investigate for optimal recovery. The viscosity of this fluid is of particular interest as it directly correlates to how pressure in the fluid flow is transduced to rotational motion of the hydraulic motor.

The working fluid must have a medium range of kinematic viscosity. Too low a viscosity, there are losses in the pressure drop across the hydraulic motor. At the same time, however, there is less shear force experienced in bends around the fluid circuit. With a high viscosity fluid, there is highly effective power transfer at the hydraulic motor end, but losses sustained in the fluid circuit due to shear forces against the tubing walls. So we take Fork Oil 5W light as our working fluid. Fork Oil 5W light has been developed for universal use.

III. RESULTS AND DISCUSSIONS

The following are the details of meshing done in ANSYS 15.0. Quad meshes are used for meshing. The meshing is done in ICEM software in ANSYS.

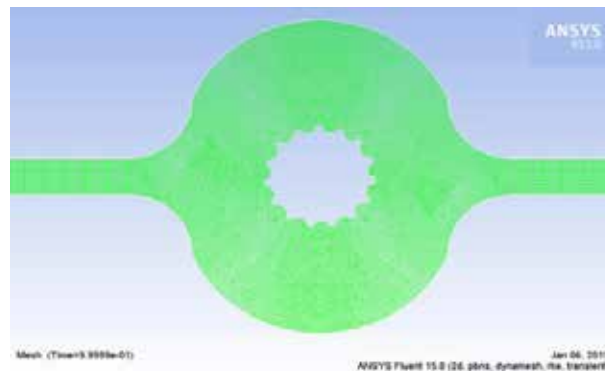


Fig. 6: Gear Meshing

3.1 Specifications

Cylinder height,	h	= 200mm
Cylinder bore diameter,	D_{bore}	= 50mm
Piston rod diameter,	D_{rod}	= 30mm
Diameter of pipe,	D_{pipe}	= 9.5mm

The material used for cylinder is mild steel and for that of piston is steel. The young's modulus of steel is 210GPa.

3.2 Contour Plots

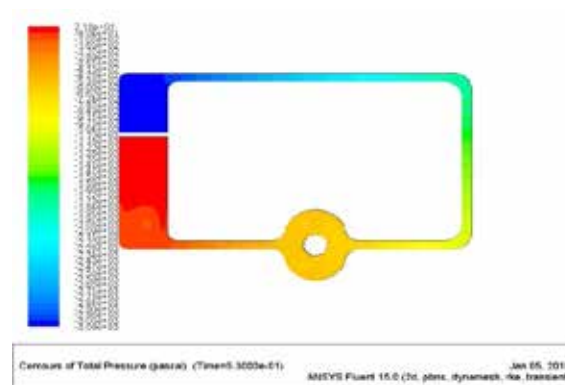


Fig. 7: Compression Stroke

Figure 7 represents the pressure at the inlet and outlet of cylinders. As mentioned above in the methodology the piston is compressed hence the fluid inside the cylinder is also compressed. Maximum compression occurs at a time of 0.53sec. From the contours so obtained we can infer that the pressure at inlet 3.9×10^3 Pa which is represented by the blue colour. At the other end the pressure is 21.8 Pa represented by the red colour. We can also infer that the pressure at inlet is the highest. This pressure is the potential driving force for the motor.

During the return stroke the piston moves back to its original position thereby compressing the fluid below the piston. This forces the fluid back into the top chamber and ready for the next cycle of operation. From the contours obtained we can infer that during compression stroke the maximum pressure obtained is 2.9×10^3 Pa represented by the blue colour. At the top chamber the pressure is 6.29 Pa represented by the red colour. During return stroke a partial vacuum is created in the top chamber which forces the liquid to flow into the chamber.

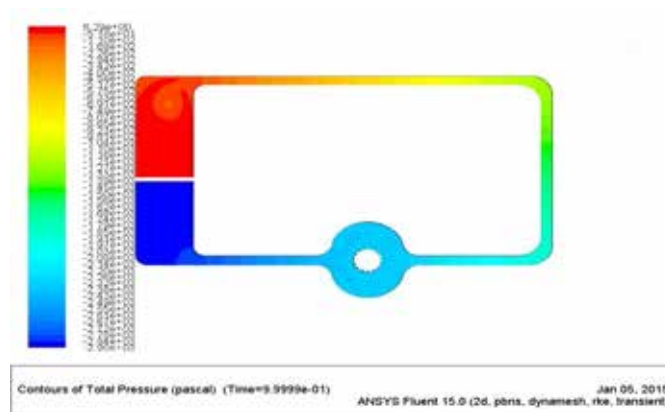


Fig. 8: Return Stroke

The above contour represents the gear velocity when the pressurised fluid from the cylinder is passed through the gear. It is this velocity that determines how much the gear rotates so that the shaft attached along the centre of gear also rotates. Neglecting the losses, it is the shafts rotation that produces the voltage when coupled with the generator. From the above contour we can infer that at inlet of gear we obtain a velocity of 0.81m/s.

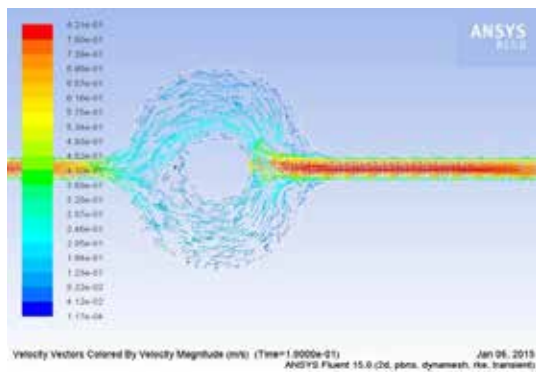


Fig. 9: Velocity of gear at 0.5Hz

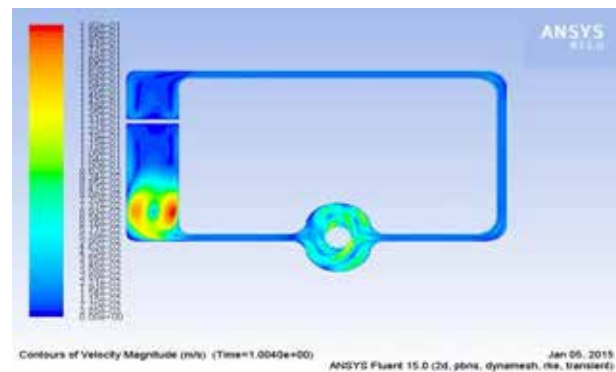


Fig. 10: Velocity of fluid at 1Hz

Within this velocity range the type of motor to be coupled with along with the shaft is low rpm motors of range 300-900 rpm. The velocity decreases along the gear part because the fluid hits the teeth of the gear pump in order to rotate it. The kinetic energy of fluid flow is used for the rotation of the gear.

The above figure shows the velocity of fluid in the cylinder when the analysis was carried for 1Hz. During compression stroke the fluid attains velocity as it passes through the gear pump and enters the bottom of cylinder.

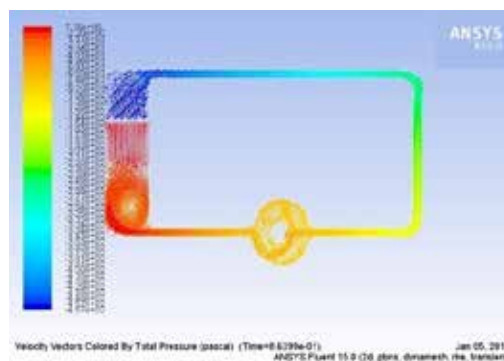


Fig. 11: Pressure at 1Hz

The above figure represents the velocity vectors along with the total pressure. We use vectorial representation for velocity. This contour is obtained by analysing the operation of damper at 1Hz.

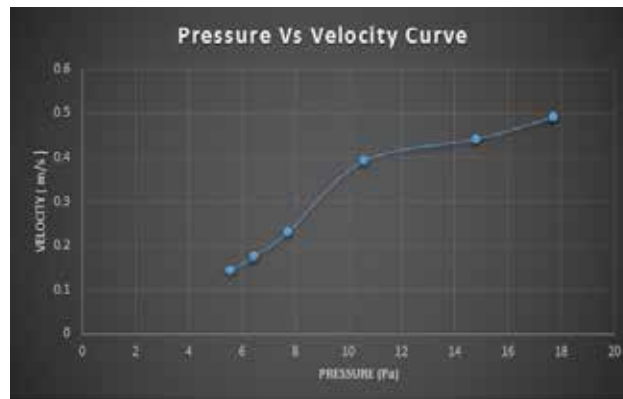


Fig. 12: Pressure velocity curve of 0.5 Hz

The Figure 12 shows the pressure Vs velocity curve obtained at 0.5 Hz. Here pressure is plotted along x-axis and velocity plotted along the y-axis. From the graph we can observe that with increase in pressure velocity increases. The values that are plotted are obtained from the analysis carried out for 0.5Hz at a time interval of 0.01sec.

IV. CONCLUSIONS

A regenerative shock absorber system is designed and analysed, which utilizes hydraulic and mechanical transmissions so that it can convert the linear motion into rotary motion to generate electricity by excitation input. A sinusoidal input has been provided so that pressure and velocity at any frequency and amplitude can be tabulated. For this purpose a user defined function (UDF) is created. From the analysis performed sufficient pressure and velocity can be achieved in order to couple a low rpm motor so as to generate electricity. Sinusoidal inputs of 0.5Hz and 1Hz is provided. A pressure Vs velocity curve is plotted and it can be seen that as pressure increases velocity also increases. With 0.5Hz and 1Hz we find that dampers designed for 1Hz has a higher pressure on the fluid. It can be concluded that different dampers can be designed for different frequency of operations.

In future, there is possibility of developing the following:

- Ø To build a prototype of the regenerative shock absorber and determine the electricity produced quantitatively.
- Ø To utilize the power so generated to run auxiliary systems experimentally.
- Ø To develop shock absorber that is capable of generating electricity during both its stroke.

REFERENCES

- [1] Babak Ebrahimi “Hybrid Electromagnetic Dampers for Vehicle Suspension Systems”, University of Waterloo, 2011.
- [2] Chuan Li and Peter W Tse, “Fabrication of an energy harvesting hydraulic damper”, Department of systems engineering and engineering management, City University of Hong Kong, China, 2013.
- [3] Ruichen Wang, Zhi Chen, Haijun Xu, Karsten Schmidt, Fengshou Gu and Andrew.D. Ball, “Modelling and Validation of a Regenerative Shock Absorber System”, Department of Computing and Engineering, Frankfurt University of Applied Sciences, Frankfurt, Germany. Proceedings of the 20th International Conference on Automation & Computing, Cranfield University, Bedfordshire, UK, 2014.